

classic) type and the late-onset (or variant) form. Clinical symptoms in classic Fabry patients are severe, and range from angiokeratomas, acroparesthesia, hypohidrosis, corneal opacity in the early teens, and progressive vascular disease of the heart, kidneys and central nervous system [2]. By contrast, patients with late-onset or variant phenotypes are usually asymptomatic until their late thirties, and their clinical manifestations are often limited to the heart [3,4] or kidneys [5]. Without medical intervention, death typically occurs in the fourth or fifth decade of life as a result of renal failure or cerebrovascular disease in classic Fabry disease [6,7], or in the fifth or sixth decade of life in variant patients who eventually suffer from heart failure or end-stage renal failure [8]. The prevalence of Fabry disease is estimated at 1 : 40 000 for the classic form. The incidence of the variant form of Fabry disease was found to be higher. Screening of various ethnic groups revealed that the incidence of cardiac variant Fabry disease among patients with unexplained hypertrophic cardiomyopathy was 3–6% [4,9], and approximately 1% of hemodialysis patients were shown to have a variant form of Fabry disease [5,10], suggesting that variant patients may be far more prevalent than previously estimated.

To date, more than 400 mutations have been identified in the  $\alpha$ -Gal A gene *GLA* (Human Gene Mutation Database Web site, <http://www.hgmd.cf.ac.uk/>). More than 57% of mutations are missense, and the majority of mutations are private, occurring only in one or a few families. The correlation between genotype and residual enzyme activity (measured primarily in leukocytes) is not strong, and presumably depends upon the nature of the mutation and additional genetic or nongenetic factors. However, the correlation between residual enzyme activity and clinical manifestations has clearly been demonstrated; higher residual enzyme activities cause mild variant phenotypes, whereas mutations that result in low residual or nondetectable enzyme activities are likely to lead to the classic phenotype [11]. Therefore, an increase in even a fraction of residual enzyme activity in patients is expected to dramatically modify disease progression and improve their quality of life.

Currently, enzyme replacement therapy (ERT) is the only effective treatment for Fabry disease. Infusion of recombinant  $\alpha$ -Gal A purified from Chinese hamster ovary cells or fibroblasts is effective in lowering the accumulation of substrate in tissues, and reduces pain in classically affected Fabry patients [12,13]. The therapy has been well tolerated by patients who revealed improvements in gastrointestinal and neurological manifestations (acroparaesthesia, hypohidrosis, and vasomotion) and quality of life [14,15]. The results of

treatment of variant Fabry patients have been mixed, suggesting that ERT may be inefficient at treating severe late-stage patients, presumably because of insufficient delivery of enzyme to particular tissues [16,17]. The therapy is expensive, which could be an economic burden for patients, especially for those living in developing countries.

An emerging therapeutic strategy using small molecules termed active-site-specific chaperones (ASSC) that are 'pharmacological chaperones' has been proposed, and is being evaluated for Fabry disease [18,19]. This strategy employs orally active molecules that are able to increase residual enzyme activity by rescuing misfolded mutant proteins from endoplasmic reticulum-associated degradation (ERAD), and promoting the smooth processing and trafficking of mutant enzymes to lysosomes. In addition to Fabry disease, small molecules capable of specifically rescuing misfolded enzyme proteins have been identified for Gaucher disease [20,21], Tay-Sachs and Sandhoff disease [22] (details for Gaucher and Tay-Sachs/Sandhoff diseases are reviewed separately), GM1-gangliosidosis [23], and retinitis pigmentosa 17 [24]. Small molecular antagonists have been identified as pharmacological chaperones for rescue of conformational defective receptors, and are reviewed elsewhere [25,26]. In this review, ASSC will be used to refer to these molecules because they are active-site directed inhibitors of the targeted enzyme. Herein, we describe a molecular basis for the deficient activity of  $\alpha$ -Gal A in mutant enzymes that are identified in Fabry patients with residual enzyme activity, and review recent progress in the development of ASSC therapy for Fabry disease. Particularly, 1-deoxygalactonojirimycin (DGJ) is explored as an example of the development of ASSC therapy.

### Structural basis of Fabry disease

The mature human  $\alpha$ -Gal A enzyme is a homodimeric glycoprotein, each monomer containing 398 amino acid residues after cleavage of the signal peptide (the first 30 amino acid residues) [27]. From X-ray crystal structural information, each monomer is composed of two domains; a  $(\beta/\alpha)_8$  domain (amino acid residues 32–330), and a C-terminal domain (residues 331–429) containing eight antiparallel  $\beta$ strands on two sheets in a  $\beta$ sandwich (Fig. 1A) [28]. The first domain contains the active-site formed by the C-terminal ends of the  $\beta$ strands at the center of a barrel. Thirteen amino acid residues were predicted to be directly involved in the interaction with  $\alpha$ -galactose. In addition, 30 residues from loops  $\beta$ 1- $\alpha$ 1,  $\beta$ 6- $\alpha$ 6,  $\beta$ 7- $\alpha$ 7,  $\beta$ 8- $\alpha$ 8,  $\beta$ 11- $\beta$ 12, and  $\beta$ 15- $\beta$ 16 of each monomer contribute

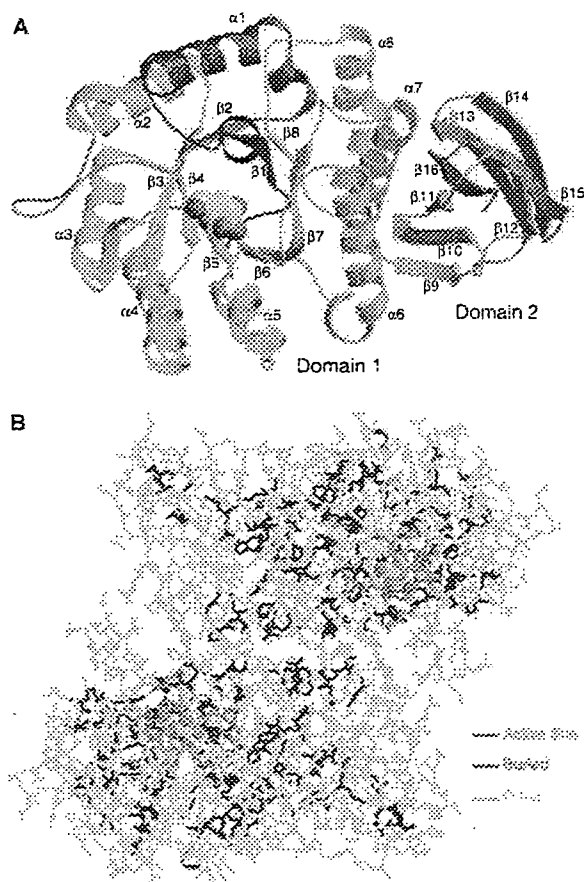


**Fig. 1.** Structure of the  $\alpha$ -Gal A monomer (A) and location of Fabry disease mutations (B). (A) The monomer is colored from the N- (blue) to C- (red) terminus. Domain 1 contains the active-site at the center of the  $\beta$ strands in the  $(\beta/\alpha)_8$  barrel, whereas domain 2 contains antiparallel  $\beta$ strands. The galactose ligand is shown in yellow and red. (B) Fabry disease-causing point mutations are shown on the human  $\alpha$ -Gal A dimer. The red, blue, and green bonds show mutations that directly perturb the active-site, involve buried residues, or fall into neither of these categories, respectively. Reproduced with permission from Garman *et al.* [28].

to the dimer interface. To understand the molecular defects responsible for Fabry disease, Garman *et al.* [28,29] mapped various missense mutations onto a model of human  $\alpha$ -Gal A (Fig. 1B). The locations of the human  $\alpha$ -Gal A point mutations reveal two major classes of Fabry disease protein defects: active-site mutations that reduce enzymatic activity by perturbing the active site without necessarily affecting the overall  $\alpha$ -Gal A structure; and folding mutations that reduce the stability of  $\alpha$ -Gal A by disrupting its hydrophobic core. It is clear that the majority of amino acids that are replaced within missense mutant proteins do not directly contribute to the enzyme's catalytic function,

but rather to the maintenance of the enzyme's tertiary structure.

### Molecular basis of the deficiency of human mutant $\alpha$ -Gal A enzymes

The deficient activity of mutant  $\alpha$ -Gal A enzymes can result from the defective biosynthesis, loss of kinetic capability, excessive degradation of mutant protein, or their combinations. During the course of examining the primary cause for deficient enzyme activity, Ishii *et al.* [30,31] examined the kinetic properties and stabilities of several mutant enzymes found in cardiac variants. Following the same approach, we recently studied various disease-causing mutations that have been identified in patients who present with residual enzyme activity regardless of clinical phenotype [32]. Sixteen mutant enzymes, including ten mutations identified in variant patients (A20P, E66Q, M72V, I91T, R112H, F113L, N215S, Q279E, M296I, and M296V), four mutations found in classic patients (E59K, A156V, L166V, and R356W), and two mutations present in both variant and classic patients (A97V and R301Q) were efficiently purified from transfected COS-7 cells, and their enzymatic and biochemical properties examined. The cardiac mutations typically present relatively higher residual enzyme activity compared to the classic mutations. Except for one mutation (E59K), all mutant proteins appeared to have normal  $K_m$  and  $V_{max}$  values, indicating that they retain full or partial catalytic activity. The  $K_m$  and  $V_{max}$  values for the E59K mutant deviated largely from those of the wild-type enzyme, indicating that this mutation causes impaired kinetic activity. Although all of the mutant enzymes examined showed the same optimal pH as the wild-type enzyme, the mutant enzymes were substantially less stable compared to the wild-type enzyme. Western blot analysis of mutant enzymes expressed in transfected COS-7 cells and patient fibroblasts demonstrated that most mutant enzymes had low protein yields, indicating that excessive degradation of the mutant enzyme could be directly responsible for deficient enzyme activity caused by these missense mutations.

In studies of intracellular trafficking and processing of mutant  $\alpha$ -Gal A enzymes, the R301Q and L166V mutant enzymes were not processed even after 24 h, as determined by a metabolic labeling and pulse-chase study [32]. The degradation of mutant protein was observed at 6 h after they were synthesized. Subcellular fractionation indicated that neither enzyme activity, nor mutant protein could be detected in the lysosomal fractions of transfected COS-7 cells. Only a small

amount of mutant enzyme activity and protein was detectable in the endoplasmic reticulum (ER)/endosomal fractions, although the protein remained unprocessed. By contrast, the kinetically impaired mutation E59K was found to be normally processed to the lysosomes in transfected COS-7 cells. These results suggested that excessive degradation of these mutant proteins occurred within the ER.

Because mutant proteins with a misfolded conformation would be subject to rapid degradation in the ERAD [33], purified mutant proteins are expected to be fully folded and have a conformation similar to that of the residual enzyme under physiological conditions. A protein with a stable conformation typically resists denaturation, whereas those proteins with a fragile conformational structure are often intolerant to thermo- or pH-denaturation. To assess conformational stability of purified mutant enzymes, we performed thermo- and pH-denaturations with these enzymes [32]. Compared to the wild-type enzyme, most mutant proteins were found to be stable only over a narrow pH range. Noticeably, the mutant proteins maintained stability similar to that of the wild-type enzyme at a pH environment similar to that in lysosomes, suggesting that the folded conformation of mutant proteins is stable in lysosomes. All mutant proteins were less stable compared to the wild-type enzyme at neutral pH. These results suggest that the substitution of an amino acid residue in missense mutant  $\alpha$ -Gal A enzymes could alter conformational stability, creating a more fragile molecular structure under neutral pH conditions.

The folding process of temporarily misfolded glycoproteins in the ER is subject to two dynamic competitive events, in which the calnexin/calreticulin system and glucosidases I and II promote refolding, whereas

ER  $\alpha$ -mannosidases and the ER degradation enhancing  $\alpha$ -mannosidase I-like protein are involved in retrotranslocation and degradation of misfolded proteins in the process of ERAD [34]. Removal of a mannose residue from Man9 N-linked oligosaccharides by ER  $\alpha$ -mannosidase I is a critical luminal event for preventing proteins from reentering the refolding process, and serves as a signal for targeted ERAD. Inhibition of ER  $\alpha$ -mannosidase I often delays the degradation of glycoproteins in the ERAD in favor of protein refolding. When kifunensine, a selective inhibitor of the ER  $\alpha$ -mannosidase I, was added to the culture medium of transfected cells, the amount of all mutant proteins (except E59K) appeared to increase (Fig. 2), suggesting that the degradation of mutant enzymes was partially inhibited. This result provided clear evidence that degradation of misfolded mutant  $\alpha$ -Gal A enzymes occurred by ERAD as the result of misfolding of mutant proteins.

Protein misfolding is recognized as an important cause of protein deficiency in various inherited disorders [35]. Despite the widespread occurrence of protein misfolding, supported by the fact that individual cases of misfolding exist in a variety of diseases, the significance of protein misfolding in each genetic disorder has not been well addressed except in a few examples, such as the  $\Delta$ F508 mutation that causes misfolding of cystic fibrosis transmembrane regulator and is responsible for the majority of cystic fibrosis patients [36]. The results obtained from a large set of Fabry missense mutant proteins also provide evidence that protein misfolding is a primary cause of protein deficiency not limited to a few mutations, but rather is a generalized pathophysiological phenomenon that occurs as the result of many missense mutations in a single

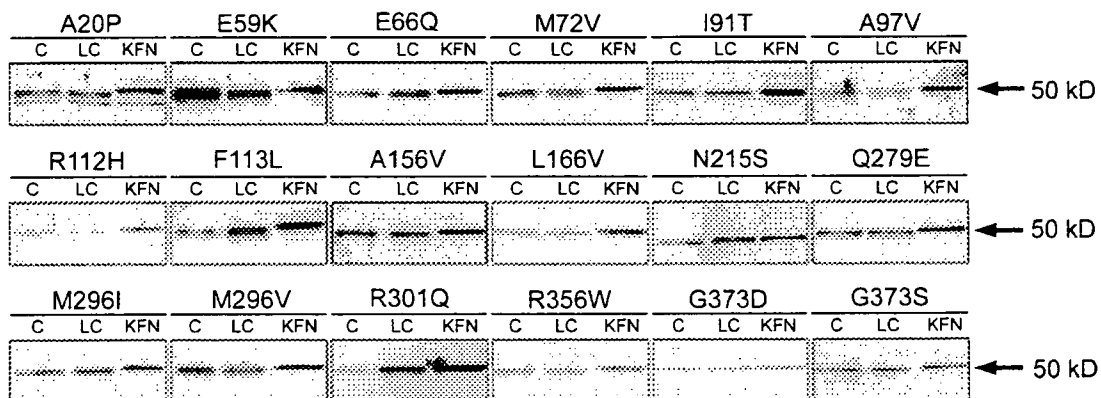


**Fig. 2.** Effects of ERAD inhibitors on the amount of mutant  $\alpha$ -Gal A expressed in COS-7 cells. Wild-type, or mutant  $\alpha$ -Gal A enzymes were transiently expressed in COS-7 cells. Cells were treated with 2  $\mu$ M lactacystin (LC), or 0.2 mM kifunensine (KFN) 5 h after transfection. Upon harvest, western blot analyses of cell lysates were performed. (C) Control. Reproduced permission from Ishii *et al.* [32].

genetic disorder. The development of strategies that specifically rescue such misfolded mutant proteins from the ERAD could be significant in battling various inherited protein deficiencies.

### Development of ASSC therapy for Fabry disease

The strategy of using competitive inhibitors as ASSCs began with DGJ for increasing residual  $\alpha$ -Gal A activity in the lymphoblasts established from Fabry patients [18,19]. Prior to this, studies of the residual activities of mutant enzymes in many Fabry patients showed that some of them had kinetic properties similar to those for wild-type  $\alpha$ -Gal A [3,30,37]. The biosynthetic processing was delayed in the cultured fibroblasts of a Fabry patient [38], and over-expressed mutant protein formed aggregates in the ER of transfected COS-1 cells [39], suggesting that enzyme deficiency in some mutants may primarily be caused by an aborted exit from the ER. Upon the realization that the deficiency of  $\alpha$ -Gal A activity could be the direct consequence of mutant protein misfolding within the ER, we purposely took a chemical biology approach to seek

active-site directed competitive inhibitors for the enhancement of residual enzyme activity. Enzyme substrates and substrate analogues have been historically used as enzyme stabilizers *in vitro*. If the hypothesis were true, potent enzyme inhibitors could serve as a folding template in the ER to modify the dynamics of protein folding in favor of proper folding, thereby increasing intracellular enzyme activity (Fig. 3). Retrospectively, these enzyme inhibitors could be useful tools for probing and assessing the folding status of a mutant protein. To gain therapeutic benefits, the rescued mutant enzyme needs to be active and free of inhibitors in the lysosomes. Competitive inhibitors have, contradictorily, potential to fulfill such requirements *in vivo*. Massive storage of glycolipid substrates would replace chaperone inhibitors in lysosomes to permit the catalytic function of enzymes. In addition, dynamic exclusion of small molecules *in vivo* could be an additional advantage in stripping off the inhibitors from the mutant enzymes. If necessary, this could be accomplished by an alternate scheduled dose in patients (e.g. a 1-week dose of the chaperone drugs to permit the accumulation of mutant enzymes in lysosomes, followed by a halt in drug administration the

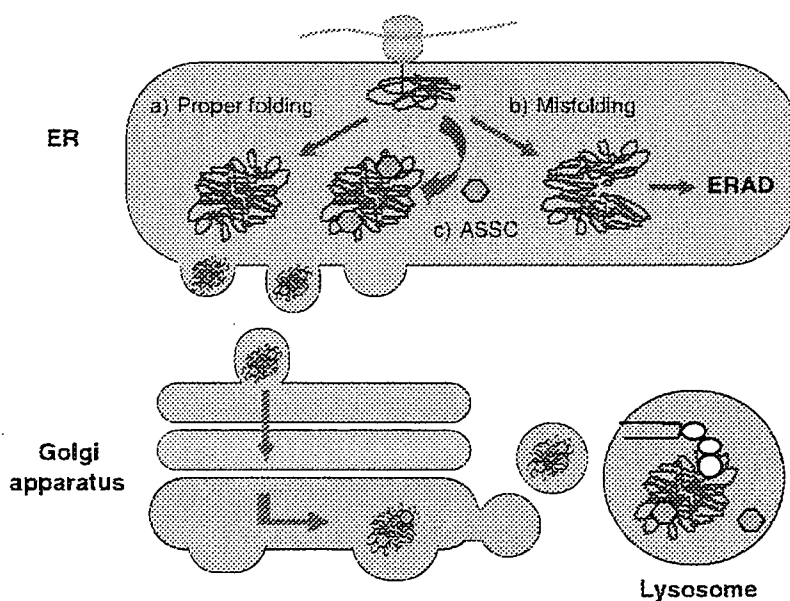


**Fig. 3.** Consequence of misfolded  $\alpha$ -Gal A in the ER and active-site-specific chaperone therapy. Synthesis of proteins takes place at ribosomes, and newly synthesized proteins are secreted to the lumen of the ER. The ER has developed a 'quality-control system' to ensure the full integrity of each protein. This system is enforced by several molecular chaperones and folding-assistant enzymes. (a) Appropriately folded proteins are transported out of the ER, whereas (b) misfolded and unfolded mutant proteins are retained in the ER and are eventually degraded by ERAD. (c) ASSCs (red hexagons) bind to the active-sites of mutant enzymes and induce their properly folded conformation. As a result, this prevents excessive degradation of the mutant proteins within ERAD and promotes their smooth transport to the Golgi apparatus. Once the mutant protein/ASSC complex reaches lysosomes, ASSCs are replaced by massive storage of substrates to allow the catalytic function of the mutant enzymes.

following week to accelerate dissociation of inhibitors from the enzymes), permitting reduction of substrate storage by the mutant enzymes. As a result, DGJ was discovered as an ASSC specifically effective for Fabry disease [18].

DGJ is a small molecular iminosugar that resembles an  $\alpha$ -galactose residue when bound to the active-site of  $\alpha$ -Gal A. DGJ is one of the most potent competitive inhibitors for  $\alpha$ -Gal A [40]. Based upon active-site interactions observed in the crystal structure of  $\alpha$ -galactose bound to  $\alpha$ -Gal A, a model of DGJ binding to  $\alpha$ -Gal A shows many favorable interactions: the imino group on DGJ is expected to interact with D170; the hydroxyl groups of DGJ form hydrogen bonds with D92, D93, K168, E203, R227, and E231; and a hydrophobic surface on DGJ makes van der Waals interactions with W47 (Fig. 4). The binding between DGJ and the protein would fix the active-site involving the five loops  $\beta$ 1- $\alpha$ 1,  $\beta$ 2- $\alpha$ 2,  $\beta$ 4- $\alpha$ 4,  $\beta$ 5- $\alpha$ 5, and  $\beta$ 6- $\alpha$ 6. The initial folding process in the ER is a thermodynamic equilibrium based upon the amino

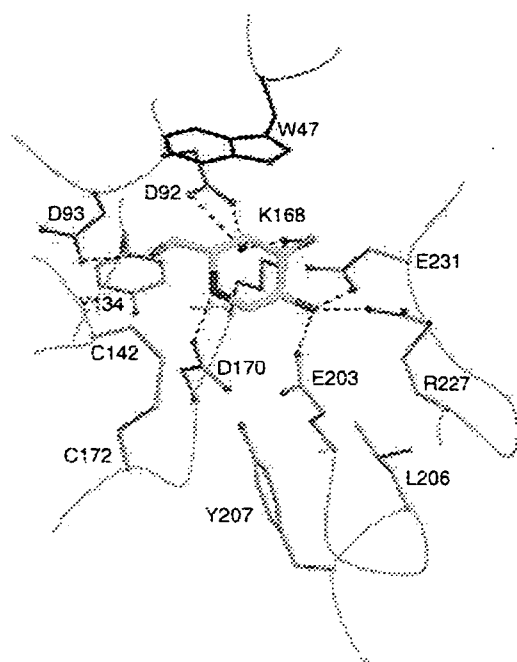


**Fig. 4.** Predicted interactions between DGJ and the active-site of  $\alpha$ -Gal A. DGJ is a known active-site directed competitive inhibitor of  $\alpha$ -Gal A. Interactions of  $\alpha$ -Gal A with DGJ were modeled based upon the crystal structure of  $\alpha$ -Gal A with bound  $\alpha$ -galactose. The key interactions with the 2-, 3-, 4-, and 6-hydroxyls on the ligand are maintained when either  $\alpha$ -galactose or DGJ bind to the active site. One key interaction between E231 on the enzyme and the anomeric hydroxyl of  $\alpha$ -galactose is lost when DGJ binds. Modified from Ishii *et al.* [32].

acid sequence of the peptide. A firm binding between DGJ and the fragile enzyme could dramatically shift the folding process toward normal folding, conferring the correct conformation on mutant enzymes that would otherwise be largely misfolded.

### Cellular enhancement of mutant $\alpha$ -Gal A activity with DGJ

ASSC activity is derived from a combination of affinity to the targeted protein, cellular permeability, and ER accessibility. An ASSC is required to cross both the plasma and ER membranes, and be deliverable to the ER where it binds to and rescues its counterpart. Although an *in vitro* enzyme inhibitory assay could be an efficient initial screening of ASSCs, a cell-based enhancement assay was performed to evaluate the ASSC activity of DGJ [41]. In an attempt to rescue misfolded mutant enzyme from excessive degradation, we demonstrated that DGJ effectively increased residual  $\alpha$ -Gal A activity in Fabry lymphoblasts derived from hemizygous Fabry patients with the R301Q or Q279E mutations. These cells were treated with concentrations lower than that usually required for intracellular inhibition of the enzyme [18,40]. The enzyme activity in R301Q or Q279E lymphoblasts increased by eight- or seven-fold, respectively, after cultivation with DGJ at 20  $\mu$ M for 4 days, and the increase was dose-dependent at concentrations that were not intracellularly inhibitory. DGJ was  $\alpha$ -Gal A specific, and did not affect misfolded mutant proteins in fibroblasts from other lysosomal storage disease patients at the concentrations effective for  $\alpha$ -Gal A [40]. Upon treatment with DGJ of transfected COS-7 cells, R301Q and L166V mutant enzymes were apparently trafficked into lysosomes in a processed mature form [32]. Independent studies by Yam *et al.* [42] in transgenic mouse fibroblasts that overexpress human R301Q  $\alpha$ -Gal A confirmed that the mutant enzyme was retained in the ER and not correctly folded, as demonstrated by the formation of complexes with BiP. Cultivation of the cells with DGJ significantly reduced these complexes, indicating that DGJ exerts a chaperone-like effect on enzyme conformation. In human Fabry R301Q and Q357X fibroblasts, DGJ treatment resulted in clearance of lysosomal storage, accompanied by the disappearance of multilamellar lysosomal inclusions. Genes involved in cell stress signaling, heat shock response, unfolded protein response, and ERAD show no apparent difference in expression between untreated and DGJ-treated fibroblasts [43], indicating that DGJ does not directly affect the ERAD system.

Schiffmann and colleagues have used a T-cell based system to determine whether the activity of 11 Fabry disease enzyme mutants can be enhanced using DGJ. When patient-derived T cells were grown in the presence of DGJ,  $\alpha$ -Gal A activity increased to more than 50% of normal for several mutations, including A97V, R112H, R112C, A143T, and L300P [44]. We recently tested DGJ enhancement in patient fibroblasts and lymphoblasts expressing a variety of disease-causing  $\alpha$ -Gal A missense mutations. The results showed that residual enzyme activity could be specifically increased 20% above normal after incubating the cultured cells with DGJ at 20  $\mu$ M for 5 days [32].

Interestingly, the effect of DGJ does not appear to be limited to mutations that primarily cause protein misfolding. After treatment with DGJ, residual enzyme activity increased by eight-fold in the cultured fibroblasts of a Fabry patient with the E59K mutation. This mutation has been shown to confer compromised kinetic properties, and protein misfolding is not a major obstacle to enzyme activity [32]. It has been proposed that retention and degradation of misfolded proteins entering the secretory pathway may not be restricted to mutant proteins [45]. Protein folding is not a perfect process even with wild-type proteins. A large fraction of newly synthesized proteins never attain their native structure, and are ubiquitinated before being degraded by cytosolic proteasomes. Small molecular ligands have also been shown to be effective at increasing maturation of the wild-type  $\delta$ -opioid receptor [46]. Evidence obtained from our study indicates that DGJ enhancement could be clinically beneficial for a broad range of missense mutations that not only cause protein misfolding, but also other types of protein defects.

### Enhancement of mutant $\alpha$ -Gal A activity with DGJ in transgenic mice

To examine the effect of DGJ enhancement *in vivo*, we generated transgenic mice expressing human mutant  $\alpha$ -Gal A (R301Q) in an endogenous null background [47]. Because the expression level of the transgene is substantially higher than that of the endogenous gene, these mice are clinically healthy, and do not present a clinical phenotype. Because the mice exclusively express human mutant enzyme in all major tissues including the heart, kidneys, and brain (the main organs affected by Fabry disease in man), they are an excellent biochemical animal model for *in vivo* proof-of-concept, and allow the pharmacokinetics of DGJ to be studied. Oral administration of DGJ to transgenic mice led a dose-dependent increase in  $\alpha$ -Gal A activity

in the major tissues of the mice. Enzyme activities increased by 13-, 3.3-, 3.9-, 2.6-, and 2.3-fold in heart, kidneys, spleen, liver, and brain, respectively, in mice that were fed with DGJ at approximately 3 mg·g<sup>-1</sup> body weight·day<sup>-1</sup> for 2 weeks [47]. No apparent toxic effects were observed in transgenic mice treated with DGJ for 140 days, indicating that DGJ is well tolerated in mice.

### ASSC therapy for Fabry disease in humans

The clinical proof-of-concept for ASSC therapy has been investigated in cardiac Fabry disease by Frustaci and colleagues [48]. Galactose, a less effective inhibitor of  $\alpha$ -Gal A compared to DGJ, was administered to a cardiac Fabry patient by intravenous infusion at 1 g·kg<sup>-1</sup> three times weekly. After a 3-month treatment period, remarkable improvements in the increase in the left ventricular ejection fraction (from 32% to 51%), and reduction in ventricular wall thickness (from 18 mm to 15 mm) were observed. The patient who had severe myocardial disease no longer required a cardiac transplant, and returned to full-time work after 2 years of treatment. Although galactose is not considered to be a viable therapeutic agent for Fabry disease because it requires an excessive amount of intravenous infusions every other day to sustain its therapeutic effect, the concept of ASSC was confirmed as an effective therapeutic approach in humans.

DGJ is approximately 120 000-fold more potent than galactose. Upon completion of preclinical safety tests in rats and monkeys, clinical phase I trials for DGJ (Amigal<sup>TM</sup>) were conducted in healthy volunteers for safety and pharmacokinetics (<http://www.amicustherapeutics.com>). Currently, several phase II clinical trials for Amigal are being conducted with male and female Fabry patients who harbor a variety of missense mutations.

### How much residual enzyme activity is enough?

A full level of lysosomal enzyme activity is not required to prevent the storage of substrate. Many lysosomal storage disease patients with a significant level of residual enzyme activity are asymptomatic, indicating that clinical symptoms develop in patients only when the level of residual enzyme activity falls to a critical threshold [49]. In Fabry disease, the critical threshold for residual enzyme activity could vary between individuals. However, based on the fact that the majority of diagnosed variant patients retain residual enzyme activity at

5–10% the level of normal, and that a hemizygote patient with less than 3% of the normal level is likely to present classic symptoms, one would assume that residual enzyme activity greater than 10% of normal in hemizygote patients might be sufficient at reducing the majority of clinical symptoms. Even for patients whose residual enzyme activity cannot be increased over approximately 10% of normal, any increase in activity is still considered to be clinically beneficial because it may dramatically modify the clinical phenotype and reduce clinical manifestations that affect quality of life.

### Perspective of DGJ treatment for Fabry disease

To date, ERT is the only available Food and Drug Administration approved therapy for Fabry disease. ERT has clear advantages in that it can be administered to a full clinical spectrum of patients, including those with nonsense mutations and missense mutations that result in total disruption of the catalytic domain. For them, DGJ would not be effective. On the other hand, DGJ is expected to be highly effective for patients who have missense mutations that primarily lead to misfolding of the mutant protein. DGJ could also be useful as an adjunct therapy with ERT for patients whose residual enzyme activity cannot be increased by DGJ alone to a level that reverses disease development. This could potentially reduce the overall therapeutic cost and add convenience for patients. Compared to the protein macromolecule that is administered through intravenous infusion every other week, DGJ is an orally active small molecule drug. This would provide undeniable advantages of convenience, cost savings, and ease of accessibility by the drug to tissues, including the central nervous system. Because a large proportion of mutant enzymes in Fabry patients with missense mutations are kinetically active, ASSC therapy using DGJ may be broadly applicable to Fabry patients with various missense mutations.

### Acknowledgements

The authors are grateful to Dr S. Garman of University of Massachusetts for providing photos of X-ray structure of  $\alpha$ -Gal A and to Dr J. Shabbeer for editorial assistance with the manuscript. This work was supported in part by research grants from the Ministry of Education, Science and Culture of Japan (S.I. and J.Q.F.), the Ministry of Health, Labour and Welfare of Japan (S.I.), Mizutani Glycoscience Foundation, Irma T. Hirschl Foundation, and American Heart Association (J.Q.F.).

### References

- 1 Brady OR, Gal AE, Bradley RM, Martensson E, Warshaw AL & Laster L (1967) Enzymatic defect in Fabry's disease: ceramidetrihexosidase deficiency. *N Engl J Med* **276**, 1163–1167.
- 2 Desnick RJ, Ioannou YA & Eng CM (2001)  $\alpha$ -galactosidase A deficiency: Fabry disease. *The Metabolic and Molecular Bases of Inherited Disease* (Scriver CR, Beaudet AL, Sly WS & Valle D, eds), pp. 3733–3774. McGraw-Hill, New York, NY.
- 3 Bishop DF, Grabowski GA & Desnick RJ (1981) Fabry disease: an asymptomatic hemizygote with significant residual  $\alpha$ -galactosidase A activity. *Am J Hum Genet* **33**, 71A.
- 4 Nakao S, Takenaka T, Maeda M, Kodama C, Tanaka A, Tahara M, Yoshida A, Kuriyama M, Hayashibe H, Sakuraba H *et al.* (1995) An atypical variant of Fabry's disease in men with left ventricular hypertrophy. *N Engl J Med* **333**, 288–293.
- 5 Nakao S, Kodama C, Takenaka T, Tanaka A, Yasumoto Y, Yoshida A, Kanzaki T, Enriquez AL, Eng CM, Tanaka H *et al.* (2003) Fabry disease: detection of undiagnosed hemodialysis patients and identification of a 'renal variant' phenotype. *Kidney Int* **64**, 801–807.
- 6 Shah JS & Elliott PM (2005) Fabry disease and the heart: an overview of the natural history and the effect of enzyme replacement therapy. *Acta Paediatr Suppl* **94**, 11–14.
- 7 Branton M, Schiffmann R & Kopp JB (2002) Natural history and treatment of renal involvement in Fabry disease. *J Am Soc Nephrol* **13** (Suppl. 2), S139–S143.
- 8 Desnick RJ, Brady R, Barranger J, Collins AJ, Germain DP, Goldman M, Grabowski G, Packman S & Wilcox WR (2003) Fabry disease, an under-recognized multisystemic disorder: expert recommendations for diagnosis, management, and enzyme replacement therapy. *Ann Intern Med* **138**, 338–346.
- 9 Sachdev B, Takenaka T, Teraguchi H, Tei C, Lee P, McKenna WJ & Elliott PM (2002) Prevalence of Anderson–Fabry disease in male patients with late onset hypertrophic cardiomyopathy. *Circulation* **105**, 1407–1411.
- 10 Bekri S, Enica A, Ghafari T, Plaza G, Champenois I, Choukroun G, Unwin R & Jaeger P (2005) Fabry disease in patients with end-stage renal failure: the potential benefits of screening. *Nephron Clin Pract* **101**, C33–C38.
- 11 Schaefer E, Mehta A & Gal A (2005) Genotype and phenotype in Fabry disease: analysis of the Fabry Outcome Survey. *Acta Paediatr Suppl* **94**, 87–92.
- 12 Eng CM, Guffon N, Wilcox WR, Germain DP, Lee P, Waldek S, Caplan L, Linthorst GE & Desnick RJ (2001) Safety and efficacy of recombinant human  $\alpha$ -galactosidase A – replacement therapy in Fabry's disease. *N Engl J Med* **345**, 9–16.

- 13 Schiffmann R, Kopp JB, Austin HA III, Sabnis S, Moore DF, Weibel T, Balow JE & Brady RO (2001) Enzyme replacement therapy in Fabry disease: a randomized controlled trial. *JAMA* **285**, 2743–2749.
- 14 Banikazemi M, Ullman T & Desnick RJ (2005) Gastrointestinal manifestations of Fabry disease: clinical response to enzyme replacement therapy. *Mol Genet Metab* **85**, 255–259.
- 15 Bongiorno MR, Pistone G & Arico M (2003) Fabry disease: enzyme replacement therapy. *J Eur Acad Dermatol Venereol* **17**, 676–679.
- 16 Tsambaos D, Chroni E, Manolis A, Monastirli A, Pasmatzi E, Sakkis T, Davlourous P, Goumenos D, Katrivanou A & Georgiou S (2004) Enzyme replacement therapy in severe Fabry disease with renal failure: a 1-year follow-up. *Acta Derm Venereol* **84**, 389–392.
- 17 Spinelli L, Pisani A, Sabbatini M, Petretta M, Andreucci MV, Procaccini D, Lo Surdo N, Federico S & Cianciaruso B (2004) Enzyme replacement therapy with agalsidase beta improves cardiac involvement in Fabry's disease. *Clin Genet* **66**, 158–165.
- 18 Fan J-Q, Ishii S, Asano N & Suzuki Y (1999) Accelerated transport and maturation of lysosomal  $\alpha$ -galactosidase A in Fabry lymphoblasts by an enzyme inhibitor. *Nat Med* **5**, 112–115.
- 19 Fan J-Q (2003) A contradictory treatment for lysosomal storage disorders: inhibitors enhance mutant enzyme activity. *Trends Pharmacol Sci* **24**, 355–360.
- 20 Sawkar AR, Cheng WC, Beutler E, Wong CH, Balch WE & Kelly JW (2002) Chemical chaperones increase the cellular activity of N370S beta-glucosidase: a therapeutic strategy for Gaucher disease. *Proc Natl Acad Sci USA* **99**, 15428–15433.
- 21 Chang HH, Asano N, Ishii S, Ichikawa Y & Fan JQ (2006) Hydrophilic iminosugar active-site-specific chaperones increase residual glucocerebrosidase activity in fibroblasts from Gaucher patients. *FEBS J* **273**, 4082–4092.
- 22 Tropak MB, Reid SP, Guiral M, Withers SG & Mahuran D (2004) Pharmacological enhancement of beta-hexosaminidase activity in fibroblasts from adult Tay-Sachs and Sandhoff Patients. *J Biol Chem* **279**, 13478–13487.
- 23 Matsuda J, Suzuki O, Oshima A, Yamamoto Y, Noguchi A, Takimoto K, Itoh M, Matsuzaki Y, Yasuda Y, Ogawa S *et al.* (2003) Chemical chaperone therapy for brain pathology in G(M1)-gangliosidosis. *Proc Natl Acad Sci USA* **100**, 15912–15917.
- 24 Bonapace G, Waheed A, Shah GN & Sly WS (2004) Chemical chaperones protect from effects of apoptosis-inducing mutation in carbonic anhydrase IV identified in retinitis pigmentosa 17. *Proc Natl Acad Sci USA* **101**, 12300–12305.
- 25 Ulloa-Aguirre A, Janovick JA, Brothers SP & Conn PM (2004) Pharmacologic rescue of conformationally defective proteins: implications for the treatment of human disease. *Traffic* **5**, 821–837.
- 26 Bernier V, Bichet DG & Bouvier M (2004) Pharmacological chaperone action on G-protein-coupled receptors. *Curr Opin Pharmacol* **4**, 528–533.
- 27 Bishop DF, Calhoun DH, Bernstein HS, Hantzopoulos P, Quinn M & Desnick RJ (1986) Human  $\alpha$ -galactosidase A: nucleotide sequence of a cDNA clone encoding the mature enzyme. *Proc Natl Acad Sci USA* **83**, 4859–4863.
- 28 Garman SC & Garboczi DN (2004) The molecular defect leading to Fabry disease: structure of human alpha-galactosidase. *J Mol Biol* **337**, 319–335.
- 29 Garman SC & Garboczi DN (2002) Structural basis of Fabry disease. *Mol Genet Metab* **77**, 3–11.
- 30 Ishii S, Kase R, Sakuraba H & Suzuki Y (1993) Characterization of a mutant  $\alpha$ -galactosidase gene product for the late-onset cardiac form of Fabry disease. *Biochem Biophys Res Comm* **197**, 1585–1589.
- 31 Ishii S, Suzuki Y & Fan J-Q (2000) Role of Ser-65 in the activity of alpha-galactosidase A: characterization of a point mutation (S65T) detected in a patient with Fabry disease. *Arch Biochem Biophys* **377**, 228–233.
- 32 Ishii S, Chang HH, Kawasaki K, Yasuda K, Wu HL, Garman SC & Fan JQ (2007) Mutant alpha-galactosidase A enzymes identified in Fabry patients with residual enzyme activity: biochemical characterization and restoration of normal intracellular processing by 1-deoxygalactonojirimycin. *Biochem J* **406**, 285–295.
- 33 Ellgaard L & Helenius A (2003) Quality control in the endoplasmic reticulum. *Nat Rev Mol Cell Biol* **4**, 181–191.
- 34 Helenius A & Aebi M (2004) Roles of N-linked glycans in the endoplasmic reticulum. *Annu Rev Biochem* **73**, 1019–1049.
- 35 Kuznetsov G & Nigam SK (1998) Folding of secretory and membrane proteins. *N Engl J Med* **339**, 1688–1695.
- 36 Welsh MJ, Ramsey BW, Accurso F & Cutting GR (2001) Cystic Fibrosis. *The Metabolic and Molecular Bases of Inherited Disease* (Scriver CR, Beaudet A, Sly WS & Valle D, eds), pp. 5121–5188. McGraw-Hill, New York, NY.
- 37 Remeo G, Urso M, Piszczane A, Blum E, de Falco A & Ruffilli A (1975) Residual activity of  $\alpha$ -galactosidase A in Fabry's disease. *Biochem Genet* **13**, 615–628.
- 38 Lemansky P, Bishop DF, Desnick RJ, Hasilik A & von Figura K (1987) Synthesis and processing of  $\alpha$ -galactosidase A in human fibroblasts. Evidence for different mutations in Fabry disease. *J Biol Chem* **262**, 2062–2065.
- 39 Ishii S, Kase R, Okumiya T, Sakuraba H & Suzuki Y (1996) Aggregation of the inactive form of human  $\alpha$ -galactosidase in the endoplasmic reticulum. *Biochem Biophys Res Commun* **220**, 812–815.



- 40 Asano N, Ishii S, Kizu H, Ikeda K, Yasuda K, Kato A, Martin OR & Fan J-Q (2000) *In vitro* inhibition and intracellular enhancement of lysosomal  $\alpha$ -galactosidase A activity in Fabry lymphoblasts by 1-deoxygalactonojirimycin and its derivatives. *Eur J Biochem* **267**, 4179–4186.
- 41 Fan JQ & Ishii S (2003) Cell-based screening of active-site specific chaperone for the treatment of Fabry disease. *Methods Enzymol* **363**, 412–420.
- 42 Yam GH, Zuber C & Roth J (2005) A synthetic chaperone corrects the trafficking defect and disease phenotype in a protein misfolding disorder. *FASEB J* **19**, 12–18.
- 43 Yam GH, Bosshard N, Zuber C, Steinmann B & Roth J (2006) Pharmacological chaperone corrects lysosomal storage in Fabry disease caused by trafficking-incompetent variants. *Am J Physiol Cell Physiol* **290**, C1076–C1082.
- 44 Shin SH, Murray GJ, Kluepfel-Stahl S, Cooney AM, Quirk JM, Schiffmann R, Brady RO & Kaneski CR (2007) Screening for pharmacological chaperones in Fabry disease. *Biochem Biophys Res Commun* **359**, 168–173.
- 45 Schubert U, Anton LC, Gibbs J, Norbury CC, Yewdell JW & Bennink JR (2000) Rapid degradation of a large fraction of newly synthesized proteins by proteasomes. *Nature* **404**, 770–774.
- 46 Petaja-Repo UE, Hogue M, Bhalla S, Laperriere A, Morello JP & Bouvier M (2002) Ligands act as pharmacological chaperones and increase the efficiency of delta opioid receptor maturation. *EMBO J* **21**, 1628–1637.
- 47 Ishii S, Yoshioka H, Mannen K, Kulkarni AB & Fan JQ (2004) Transgenic mouse expressing human mutant alpha-galactosidase A in an endogenous enzyme deficient background: a biochemical animal model for studying active-site specific chaperone therapy for Fabry disease. *Biochim Biophys Acta* **1690**, 250–257.
- 48 Frustaci A, Chimenti C, Ricci R, Natale L, Russo MA, Pieroni M, Eng CM & Desnick RJ (2001) Improvement in cardiac function in the cardiac variant of Fabry's disease with galactose-infusion therapy. *N Engl J Med* **345**, 25–32.
- 49 Leinekugel P, Michel S, Conzelmann E & Sandhoff K (1992) Quantitative correlation between the residual activity of beta-hexosaminidase A and arylsulfatase A and the severity of the resulting lysosomal storage disease. *Hum Genet* **88**, 513–523.

# Chemical Chaperone Therapy: Clinical Effect in Murine G<sub>M1</sub>-Gangliosidosis

Yoshiyuki Suzuki, MD,<sup>1</sup> Satoshi Ichinomiya, MS,<sup>1</sup> Mieko Kurosawa, PhD,<sup>2</sup> Masato Ohkubo, MD,<sup>2</sup> Hiroshi Watanabe, MD,<sup>3</sup> Hiroyuki Iwasaki, MD,<sup>3</sup> Junichiro Matsuda, PhD,<sup>4</sup> Yoko Noguchi, AS,<sup>4</sup> Kazuhiro Takimoto, PhD,<sup>5</sup> Masayuki Itoh, MD,<sup>6</sup> Miho Tabe, BS,<sup>7</sup> Masami Iida, PhD,<sup>8</sup> Takatoshi Kubo, MS,<sup>8</sup> Seiichiro Ogawa, PhD,<sup>9</sup> Eiji Nanba, MD,<sup>10</sup> Katsumi Higaki, PhD,<sup>10</sup> Kousaku Ohno, MD,<sup>11</sup> and Roscoe O. Brady, MD<sup>12</sup>

Certain low-molecular-weight substrate analogs act both as in vitro competitive inhibitors of lysosomal hydrolases and as intracellular enhancers (chemical chaperones) by stabilization of mutant proteins. In this study, we performed oral administration of a chaperone compound *N*-octyl-4-epi- $\beta$ -valienamine to G<sub>M1</sub>-gangliosidosis model mice expressing R201C mutant human  $\beta$ -galactosidase. A newly developed neurological scoring system was used for clinical assessment. *N*-Octyl-4-epi- $\beta$ -valienamine was delivered rapidly to the brain, increased  $\beta$ -galactosidase activity, decreased ganglioside G<sub>M1</sub>, and prevented neurological deterioration within a few months. No adverse effect was observed during this experiment. *N*-Octyl-4-epi- $\beta$ -valienamine will be useful for chemical chaperone therapy of human G<sub>M1</sub>-gangliosidosis.

Ann Neurol 2007;62:671–675

G<sub>M1</sub>-gangliosidosis (OMIM 230500) is a hereditary human disorder with progressive central nervous system damage, visceromegaly, and skeletal dysplasias in children and adults, caused by mutations of the gene *GLB1* (3p21.33) coding for lysosomal  $\beta$ -galactosidase (EC 3.2.1.23) that catalyzes hydrolysis of ganglioside G<sub>M1</sub> and related compounds.<sup>1</sup>

In 2003, we proposed chemical chaperone therapy

for brain pathology in G<sub>M1</sub>-gangliosidosis.<sup>2</sup> The first original studies in this direction had been published on mutant  $\alpha$ -galactosidase A in Fabry's disease, using galactose<sup>3</sup> and 1-deoxygalactonojirimycin.<sup>4</sup> We then found *N*-octyl-4-epi- $\beta$ -valienamine (NOEV) as a potent stabilizer of mutant  $\beta$ -galactosidase activity in G<sub>M1</sub>-gangliosidosis.<sup>2</sup> It increased mutant  $\beta$ -galactosidase activity in cultured fibroblasts from more than 30% of patients.<sup>5</sup>

On the other hand, we developed a novel method to assess neurological alterations in G<sub>M1</sub>-gangliosidosis model mice by modifying neurological tests in human infants and young children.<sup>6</sup> This technique was applied to monitor their clinical course under chaperone treatment. We found that NOEV prevents neurological deterioration in this animal model.

## Materials and Methods

### *G<sub>M1</sub>-Gangliosidosis Model Mice*

We maintained a C57BL/6-based congenic knock-out (KO) mouse strain with  $\beta$ -galactosidase deficiency<sup>7</sup> and a transgenic (Tg) mouse strain overexpressing R201C mutant human  $\beta$ -galactosidase.<sup>2</sup> Care of experimental animals was performed in accordance with the Guidelines on Animal Experimentation of International University of Health and Welfare (Otawara, Japan). Wild-type (WT) mice (C57BL/6Cr) were purchased from Japan SLC (Shizuoka, Japan).

### *Neurological Assessment*

Quantitative neurological assessment consisted of 11 test items.<sup>6</sup> Each item was scored in four grades (0–3) based on increasing severity of abnormality. The total scores were periodically followed. Reliability and reproducibility of this test method have been established.<sup>6</sup>

### *N-Octyl-4-epi- $\beta$ -valienamine Administration and Determination*

Tg or WT mice were provided 1mM aqueous solution of NOEV hydrochloride ad libitum. The average daily intake of NOEV was 75 $\mu$ g/gm (75mg/kg) body weight. The NOEV concentration was determined by combined liquid chroma-

From the <sup>1</sup>Graduate School, <sup>2</sup>Center for Medical Science, and <sup>3</sup>Clinical Research Center, International University of Health and Welfare, Otawara; <sup>4</sup>Biological Resource Division, National Institute of Biomedical Innovation, Ibaraki City, Osaka; <sup>5</sup>Division of Experimental Animal Research, National Institute of Infectious Diseases, Shinjuku-ku, Tokyo; <sup>6</sup>Department of Mental Retardation and Birth Defect Research, National Institute of Neuroscience, National Center of Neurology and Psychiatry, Kodaira, Tokyo; <sup>7</sup>Biochemistry Section, Analysis Center for Medical Science, SRL Inc, Hachioji; <sup>8</sup>Central Research Laboratories, Seikagaku Corporation, Higashi-Yamato, Tokyo; <sup>9</sup>Department of Biosciences and Informatics, Faculty of Science and Technology, Keio University, Kohoku-ku, Yokohama; <sup>10</sup>Division of Functional Genomics, Research Center for Bioscience and Technology, Tottori University; <sup>11</sup>Division of Child Neurology, Tottori University Faculty of Medicine, Yonago, Japan; and <sup>12</sup>Developmental and Metabolic Neurology Branch, National Institute of Neurological Disorders and Stroke, National Institutes of Health, Bethesda, MD.

Received Jul 25, 2007, and in revised form Sep 18. Accepted for publication Sep 28, 2007.

Current address for Dr Watanabe, Division of Neuronal Network, Institute of Medical Science, The University of Tokyo, Tokyo 108-8639, Japan.

Current address for Dr Iwasaki, National Rehabilitation Center for Disabled Children, Tokyo 173-0037, Japan.

This article includes supplementary material available via the Internet at <http://www.interscience.wiley.com/jpages/0364-5134/suppmat>

Published online Nov 9, 2007, in Wiley InterScience ([www.interscience.wiley.com](http://www.interscience.wiley.com)). DOI: 10.1002/ana.21284

Address correspondence to Dr Suzuki, International University of Health and Welfare Graduate School, Room L-423, 2600-1 Kitakanemaru, Otawara 324-8501, Japan. E-mail: [suzuki@iuhw.ac.jp](mailto:suzuki@iuhw.ac.jp)

tography and tandem mass spectrometry system (Fig 1). For neurological assessment, 16 Tg mice were given NOEV from 2 months of age, and they were compared clinically with the other 16 Tg mice without NOEV treatment.

#### General Pathology, Neuropathology, and Quantitative Immunohistochemistry

The mice were perfused through the heart with 4% phosphate-buffered paraformaldehyde, and tissues were used for pathology and immunohistochemistry.<sup>2,8</sup> We further performed immunohistochemical quantitation of ganglioside G<sub>M1</sub> in the brain by confocal fluorometry (Fig 2).

#### Enzyme Assay

$\beta$ -Galactosidase and  $\alpha$ -galactosidase A were assayed with 4-methylumbelliferyl derivatives (Nacalai Tesque, Kyoto) as substrates<sup>9</sup> and galactosylceramidase with 6-hexadecanoylamino-4-methylumbelliferyl  $\beta$ -galactoside (Erasmus MC, Rotterdam, the Netherlands).<sup>10</sup> Protein was determined with Micro TP-Test Wako (Wako Pure Chemical Industries, Osaka, Japan).

#### Blood Chemistry and Urinalysis

Blood was collected by cardiac puncture and centrifuged. Plasma was analyzed using FUJI DRI-CHEM 3000V (Fuji Film, Tokyo, Japan) for 14 test items, including glutamic-oxalacetic transaminase, glutamic-pyruvic transaminase, and others, as indicated by this analysis kit. Urine was performed by collection by external pressure or direct puncture of the bladder, using Uro-Labstix SG-L (Bayer Medical, Tokyo, Japan).

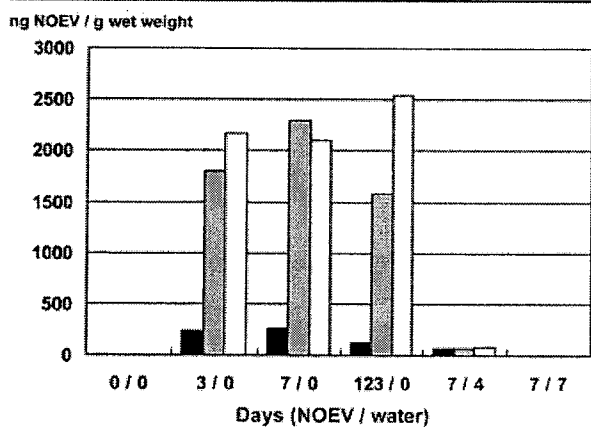


Fig 1. N-Octyl-4-epi- $\beta$ -valienamine (NOEV) concentrations in mouse tissues. Black bars indicate brain; gray bars indicate liver; white bars indicate kidney. Tissue content is measured in ng/gm wet weight. 0/0: water only (n = 2); 3/0: NOEV for 3 days (n = 2); 7/0: NOEV for 7 days (n = 2); 123/0: NOEV for 123 days (n = 1); 7/4: NOEV for 7 days, followed by water for 4 days (n = 2); 7/7: NOEV for 7 days, followed by water for 7 days (n = 2).

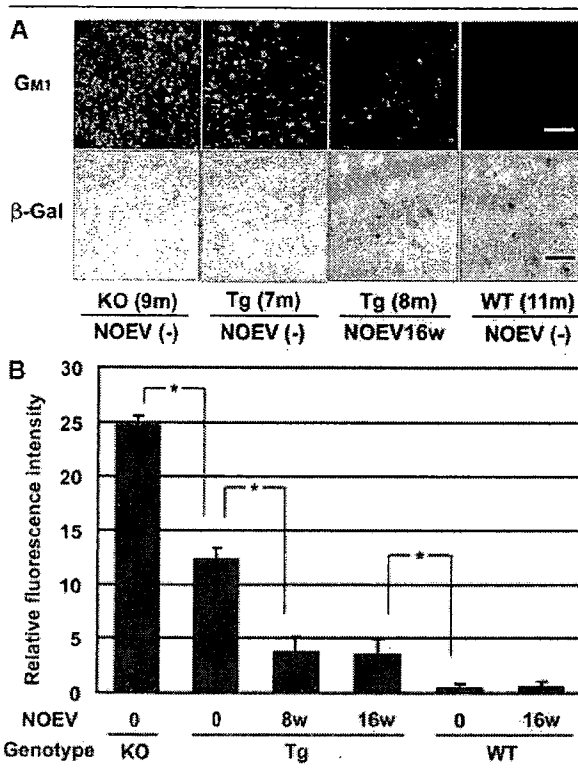


Fig 2. Immunohistochemical analysis of the R201C mouse brain. (A) Histochemical stain of G<sub>M1</sub> and  $\beta$ -galactosidase. (B) Quantitative confocal immunohistochemistry of G<sub>M1</sub>. Each column indicates the mean of relative fluorescence intensity in the mouse brain (vertical bar = standard error of the mean). \*p < 0.05. KO (0w) = KO mouse; water only (n = 2; age: 7 and 9 months). Tg (0w) = Tg mouse; water only (n = 3; age = 7, 11, and 15 months). Tg (8w) = Tg mouse; N-octyl-4-epi- $\beta$ -valienamine (NOEV) for 8 weeks (n = 2; age = 10 and 11 months). Tg (16w) = Tg mouse; NOEV for 16 weeks (n = 1; age = 9 months). WT (0w) = WT mouse; water only (n = 1; age = 11 weeks). WT (16w) = WT mouse; NOEV for 16 weeks (n = 1; age = 9 months). KO = knock-out; Tg = transgenic; WT = wild type. See supplementary material for additional methodology details.

## Results

### N-Octyl-4-epi- $\beta$ -valienamine Concentration in Mouse Tissues

The NOEV concentration increased in the brain, liver, and kidney of WT mice within 3 days immediately after starting treatment, remained at the same level for as long as 123 days of continuous administration, decreased rapidly within 4 days after discontinuation of treatment, and completely disappeared within 7 days (see Fig 1). The concentration was almost the same in the liver and kidney, and about 10% to 15% in the brain compared with the two extraneural tissues. Tissue concentrations remained the same after 8 to 16 weeks of NOEV administration in Tg mice (data not shown).

### Pathology and Immunohistochemistry

There were no specific changes in the liver, spleen, kidney, lung, heart, thymus, pancreas, or skeletal muscle of NOEV-treated mice. Bleeding, hemostasis, leukocyte infiltration, or cytoplasmic vacuolation was observed in some sporadic WT, Tg, or KO mice with or without treatment (data not shown). Immunohistochemical stain showed a marked decrease in  $G_{M1}$  storage and increase in the enzyme activity in almost all areas of the brain after 8 to 16 weeks of NOEV treatment (see Fig 2A). This observation was confirmed quantitatively by confocal fluorometry, indicating a significant decrease of  $G_{M1}$  in the NOEV-treated Tg mouse brain (see Fig 2B).

### Enzyme Activities

$\beta$ -Galactosidase activity increased remarkably during NOEV treatment for 8 to 16 weeks in Tg mice, particularly in the liver and spleen (data not shown). In the brain, the enzyme activity in Tg mice reached 30% to 40% of that in WT mice. Galactosylceramidase and  $\alpha$ -galactosidase A activities did not change in this experiment.

### Neurological Assessment

We first compared the three genotypes without NOEV treatment (Fig 3A). The total score remained low (<5) in the WT mouse until 24 months. It was high (almost 10) in the KO mouse already at 5 months (middle symptomatic stage), and increased to 25 at 9 to 10 months (late stage). The Tg mouse showed slower progression than the KO mouse. However, even at 2 to 4 months (early symptomatic stage), the mean of total score was significantly greater than that of the WT mouse.

NOEV treatment was started at 2 months of age (see Fig 3B). There was no significant difference for the first 2 months between the two groups with or without treatment. Then a definite statistical difference was detected at 5 to 7 months of age, although the score increased gradually also in the treatment group. This clinical benefit was not evident when the treatment was started at 5 months over the ensuing 5 months (data not shown).

### Blood Chemistry and Urinalysis

Glutamic-oxalacetic transaminase and glutamic-pyruvic transaminase were high in some WT, Tg, or KO mice examined. However, they were not related to the genotype, clinical course, age, or NOEV treatment. Urinalysis was normal in all mice examined.

### Discussion

In this study, we investigated the clinical effect of the chemical chaperone NOEV after our first report on laboratory data in  $G_{M1}$ -gangliosidosis mouse model.<sup>2</sup>

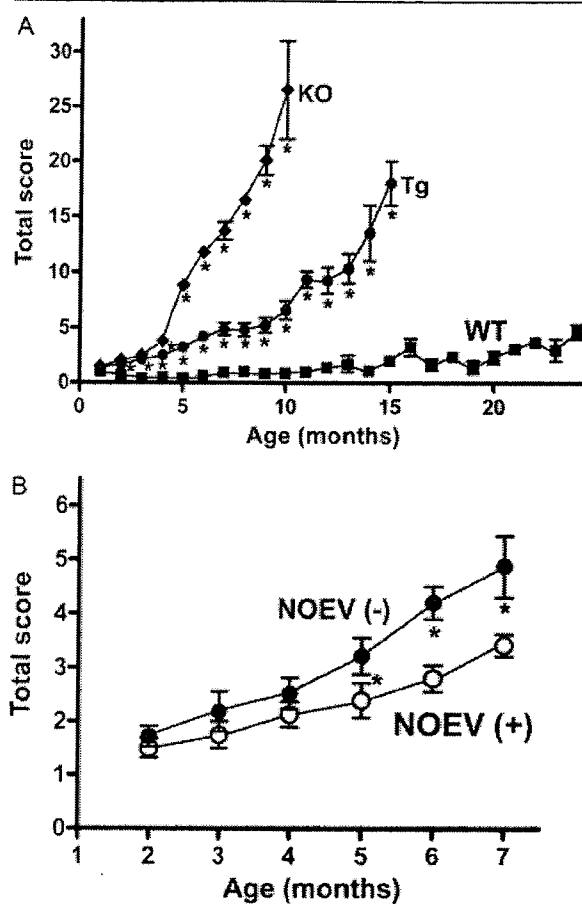


Fig 3. Neurological assessment scores in  $G_{M1}$ -gangliosidosis mouse model. (A) Clinical course in three mouse genotypes without N-octyl-4-epi- $\beta$ -valienamine (NOEV) treatment. The quantitative neurological assessment consisted of the following 11 test items: gait, posture/forelimb, posture/hind limb, posture/trunk, posture/tail, avoidance response, rolling over, body righting acting on head, parachute reflex, horizontal wire netting (stepping through interstice), and vertical wire netting (clinging and holding body).<sup>6</sup> The mice were scored in four grades based on increasing severity of abnormality for each test item: 0 (normal), 1 (slightly abnormal), 2 (moderately abnormal), and 3 (severely abnormal). The highest score was 33 for those with the most extensive neurological abnormalities. We used GraphPad Prism 4 (GraphPad Software, San Diego, CA) for unpaired Student's *t* test. Black squares indicate wild-type (WT) mouse; black circles indicate transgenic (Tg) mouse; black diamonds indicate knock-out (KO) mouse. Vertical bars indicate standard error of the mean (SEM). \**p* < 0.05 (WT vs Tg, and Tg vs KO). *n* = 10, 10, 11, 24, 28, 17, 21, 13, 2 for KO (2–10 months); *n* = 32, 11, 19, 18, 29, 17, 17, 18, 18, 17, 11, 6, 4, 2 for Tg (2–15 months); *n* = 11, 5, 12, 12, 9, 18, 21, 21, 16, 19, 18, 8, 10, 9, 11, 9, 8, 9, 9, 10, 7, 2, 3 for WT (2–24 months). (B) Clinical effect of NOEV therapy in Tg mice. The experimental conditions were the same as Figure 3A. Black circles indicate Tg mouse, nontreated; white circles indicate Tg mouse, treated with NOEV. Vertical bars indicate SEM. \**p* < 0.05. *n* = 16 for both treated and nontreated mice.

NOEV is an epimer of *N*-octyl- $\beta$ -valienamine,<sup>11,12</sup> a potent inhibitor of  $\beta$ -galactosidase in vitro<sup>13,14</sup> and a potent inducer to express mutant  $\beta$ -galactosidase activity in human and murine fibroblasts and tissues.<sup>2</sup> NOEV was effective in almost all patients with juvenile  $G_{M1}$ -gangliosidosis and in some with infantile  $G_{M1}$ -gangliosidosis.<sup>5</sup> Most patients were compound heterozygotes. We expect a successful therapeutic effect if one of the mutant genes is responsive to NOEV. The efficacy of enhancement varied among different mutations. Eight human mutant enzymes responded positively to NOEV, including known common mutations (K. Higaki and colleagues, unpublished data). The optimal NOEV concentration was 0.2  $\mu$ M for R457Q and 2  $\mu$ M for R201C and R201H.<sup>5</sup> We estimate that NOEV therapy will be successful in at least one-third of patients with  $G_{M1}$ -gangliosidosis.

This study indicates that orally administered NOEV entered the central nervous system from the bloodstream across the blood-brain barrier. The compound did not accumulate in the tissues examined during oral administration for 4 months. The increase of  $\beta$ -galactosidase activity and reduction of  $G_{M1}$  reflected changes of NOEV concentration in mouse tissues. We did not analyze urinary oligosaccharides.

In this study, we tried two new approaches for quantitative evaluation of the NOEV effect in murine  $G_{M1}$ -gangliosidosis: immunohistochemistry and clinical assessment. Quantitative confocal fluorometry demonstrated a remarkable decrease of  $G_{M1}$  in the mouse brain after NOEV treatment. The neurological assessment scores corresponded well with laboratory data.

Early chaperone therapy resulted in a positive clinical effect within a few months, although complete arrest or prevention of disease progression was not achieved under the current experimental conditions. The latency before the clinical effect was longer if the therapy was started in the late symptomatic stage. We conclude that early treatment at the early stage of disease is mandatory for prevention of brain damage. We do not know the optimal dose of NOEV at present in murine  $G_{M1}$ -gangliosidosis.

No significant adverse effect was observed during NOEV administration up to 6 months. Random increases of plasma glutamic-oxalacetic transaminase and glutamic-pyruvic transaminase concentrations were not related to genotype or NOEV treatment. Blood collection by direct cardiac puncture after ethyl ether anesthesia and thoracotomy may have partly contributed to abnormal release of intracellular enzymes into the extracellular fluid. We did not observe excessive enzyme enhancement in the course of NOEV treatment, but it may cause some metabolic derangement in human and mouse tissues.

So far we demonstrated effectiveness of chemical chaperone therapy in  $G_{M1}$ -gangliosidosis,<sup>2,5</sup> Gaucher's

disease,<sup>15,16</sup> and Fabry's disease.<sup>4</sup> A short-term effect was reported on a Fabry's disease patient with galactose,<sup>17</sup> and other investigators confirmed the effectiveness of chaperone therapy in Gaucher's disease fibroblasts.<sup>18</sup> In addition, the effect of chaperone treatment has been reported in  $G_{M2}$ -gangliosidosis<sup>19</sup> and Pompe's disease.<sup>20</sup> Theoretically, this principle can be applied to other lysosomal diseases, if a specific chaperone compound becomes available for each target enzyme. Furthermore, other neurogenetic diseases may be considered for chemical chaperone therapy. We expect that studies in this direction will open a new aspect of molecular therapy for inherited metabolic diseases with central nervous system involvement in the near future.

---

This research was supported by the Ministry of Education, Culture, Science, Sports, and Technology of Japan (13680918, 14207106, 16300141) and the Ministry of Health, Labour and Welfare of Japan (H10-No-006, H14-Kokoro-017, H17-Kokoro-019) (all grants to Y.S.).

---

## References

1. Suzuki Y, Nanba E, Matsuda J, Oshima A.  $\beta$ -Galactosidase deficiency ( $\beta$ -galactosidosis):  $G_{M1}$ -gangliosidosis and Morquio B disease. In: Scriver CR, Beaudet AL, Sly WS, et al., eds. The online metabolic and molecular bases of inherited disease. New York: McGraw-Hill, 2006. Available at: <http://genetics.accessmedicine.com>.
2. Matsuda J, Suzuki O, Oshima A, et al. Chemical chaperone therapy for brain pathology in  $G_{M1}$ -gangliosidosis. *Proc Natl Acad Sci USA* 2003;100:15912-15917.
3. Okumiya T, Ishii S, Takenaka T, et al. Galactose stabilizes various missense mutants of  $\alpha$ -galactosidase in Fabry disease. *Biochem Biophys Res Commun* 1995;214:1219-1224.
4. Fan J, Ishii S, Asano N, Suzuki Y. Accelerated transport and maturation of lysosomal  $\alpha$ -galactosidase A in Fabry lymphoblasts by an enzyme inhibitor. *Nat Med* 1999;5:112-115.
5. Iwasaki H, Watanabe H, Iida M, et al. Fibroblast screening for chaperone therapy in  $\beta$ -galactosidosis. *Brain Dev* 2006;28:482-486.
6. Ichinomiya S, Watanabe H, Maruyama K, et al. Neurological assessment of  $G_{M1}$ -gangliosidosis model mice. *Brain Dev* 2006;29:210-216.
7. Matsuda J, Suzuki O, Oshima A, et al.  $\beta$ -Galactosidase-deficient mouse as an animal model for  $G_{M1}$ -gangliosidosis. *Glycoconj J* 1997;14:729-736.
8. Itoh M, Matsuda J, Suzuki O, et al. Development of lysosomal storage in mice with targeted disruption of the  $\beta$ -galactosidase gene: a model of human  $G_{M1}$ -gangliosidosis. *Brain Dev* 2001;23:379-384.
9. Sakuraba H, Aoyagi T, Suzuki Y. Galactosialidosis ( $\beta$ -galactosidase neuraminidase deficiency): a possible role of serine thiol proteases in the degradation of  $\beta$ -galactosidase molecules. *Clin Chim Acta* 1982;125:275-282.
10. Wiederschain G, Raghavan S, Kolodny E. Characterization of 6-hexadecanoylamino-4-methylumbelliferyl- $\beta$ -D-galactopyranoside as fluorogenic substrate of galactocerebrosidase for the diagnosis of Krabbe disease. *Clin Chim Acta* 1992;205:87-96.
11. Ogawa S, Ashiura M, Uchida C, et al. Synthesis of potent  $\beta$ -D-glucocerebrosidase inhibitors: *N*-alkyl- $\beta$ -valienamines. *Bioorg Med Chem Lett* 1996;6:929-932.

12. Ogawa S, Kobayashi E, Kabayama K, et al. Chemical modification of  $\beta$ -glucocerebrosidase inhibitor N-octyl- $\beta$ -valienamine: synthesis and biological evaluation of N-alkanoyl and N-alkyl derivatives. *Bioorg Med Chem* 1998;6:1955–1962.
13. Ogawa S, Kobayashi-Matsunaga Y, Suzuki Y. Chemical modification of the  $\beta$ -glucocerebrosidase inhibitor N-octyl- $\beta$ -valienamine: Synthesis and biological evaluation of 4-epimeric and 4-O-( $\beta$ -D-galactopyranosyl) derivatives. *Bioorg Med Chem* 2002;10:1967–1972.
14. Ogawa S, Sakata Y, Ito N, et al. Convenient synthesis and evaluation of glycosidase inhibitory activity of  $\alpha$ - and  $\beta$ -galactose-type valienamines, and some N-alkyl derivatives. *Bioorg Med Chem* 2004;12:995–1002.
15. Lin H, Sugimoto Y, Ohsaki Y, et al. N-Octyl- $\beta$ -valienamine up-regulates activity of F213I mutant  $\beta$ -glucosidase in cultured cells: a potential chemical chaperone therapy for Gaucher disease. *Biochim Biophys Acta* 2004;1689:219–228.
16. Lei K, Ninomiya H, Suzuki M, et al. Enzyme enhancement activity of N-octyl- $\beta$ -valienamine on  $\beta$ -glucosidase mutants associated with Gaucher disease. *Biochim Biophys Acta* 2007;1772:587–596.
17. Frustaci A, Chimenti C, Ricci R, et al. Improvement in cardiac function in the cardiac variant of Fabry's disease with galactose-infusion therapy. *N Engl J Med* 2001;345:25–32.
18. Sawkar A, Cheng W, Beutler E, et al. Chemical chaperones increase the cellular activity of N370S  $\beta$ -glucosidase: a therapeutic strategy for Gaucher disease. *Proc Natl Acad Sci USA* 2002;99:15428–15433.
19. Tropak M, Reid S, Guiral M, et al. Pharmacological enhancement of  $\beta$ -hexosaminidase activity in fibroblasts from adult Tay-Sachs and Sandhoff patients. *J Biol Chem* 2004;279:13478–13487.
20. Parenti G, Zuppaldi A, Gabriela P, et al. Pharmacological enhancement of mutated  $\alpha$ -glucosidase activity in fibroblasts from patients with Pompe disease. *Mol Ther* 2007;15:508–514.

# Development and Medical Application of Unsaturated Carboglycosylamine Glycosidase Inhibitors

Seiichiro Ogawa<sup>a,\*</sup>, Miki Kanto<sup>a</sup> and Yoshiyuki Suzuki<sup>b,\*</sup>

<sup>a</sup>Department of Biosciences and Informatics, Faculty of Science and Technology, Keio University, Hiyoshi, Kohoku-ku, Yokohama, 223-8522 Japan; <sup>b</sup>International University of Health and Welfare Graduate School, Kita-Kanemaru, Otawara, 324-8501 Japan

**Abstract:** This article reviews synthesis and structures of carboglycosylamines, a group of carbocyclic sugar analogues. Some unsaturated derivatives are known to be potent glycosidase inhibitors. Among them, *N*-octyl-4-epi- $\beta$ -valienamine as a lysosomal  $\beta$ -galactosidase inhibitor is currently undergoing a new molecular therapeutic trial (chemical chaperone therapy) for control of the human  $\beta$ -galactosidase deficiency disorder, GM1-gangliosidosis.

**Key Words:** Carbasugars, aminocyclitols, 5a-carboglycosylamines, glycosidase inhibitors, chemical chaperone therapy, lysosomal disease, GM1-gangliosidosis.

## 1. INTRODUCTION

Inhibition of glycosidases may be useful for treatment of diseases [1] such as diabetes, viral and bacterial infections, and inflammation. Among currently important glycosidase inhibitors, validamycin A (1) [2] and acarbose (2) [3], widely used to control sheath bright of rice plant and to treat diabetes, respectively, feature the same unsaturated branched-chain aminocyclitol, valienamine [4] (**4 $\alpha$** ), with a glycoside-like N-linked bond (Fig. 1). Other related compounds are components of validamycins: validamine (**3 $\alpha$** ) and valioline (**5 $\alpha$** ). They belong to carbasugars [6], carbocyclic analogues of glycofuranoses and pyranoses, where the ring-oxygen atoms are replaced with carbon atoms. The valienamine-1 and 2 have been shown to play roles by structural mimicking of transition states of glucopyranose residues during hydrolysis of glucosides [6] (Fig. 2), binding to the active sites of enzymes. Compounds **3 $\alpha$** –**5 $\alpha$**  themselves possess more or less notable inhibitory activity toward glycohydrolases. Actually, further development of strong and specific  $\alpha$ -glucosidase inhibitors has been carried out extensively through their chemical modification, leading to discovery of voglibose [7], a clinically important medicine for treatment of diabetes, fully compatible with acarbose (2) (Fig. 3). Since then, unfortunately, only very few studies have so far been directed toward these compounds, compared with those on aza sugar glycosidase inhibitors, viz. 1-deoxynojirimycin (DNJ) and related compounds. This situation has thus stimulated our interest in identifying new type of carboglycosylamine glycosidase inhibitors as therapeutic agents, taking advantage of their structural and biochemical features.

Surprisingly some of these *in vitro* inhibitors were found to induce remarkable expression of mutant lysosomal

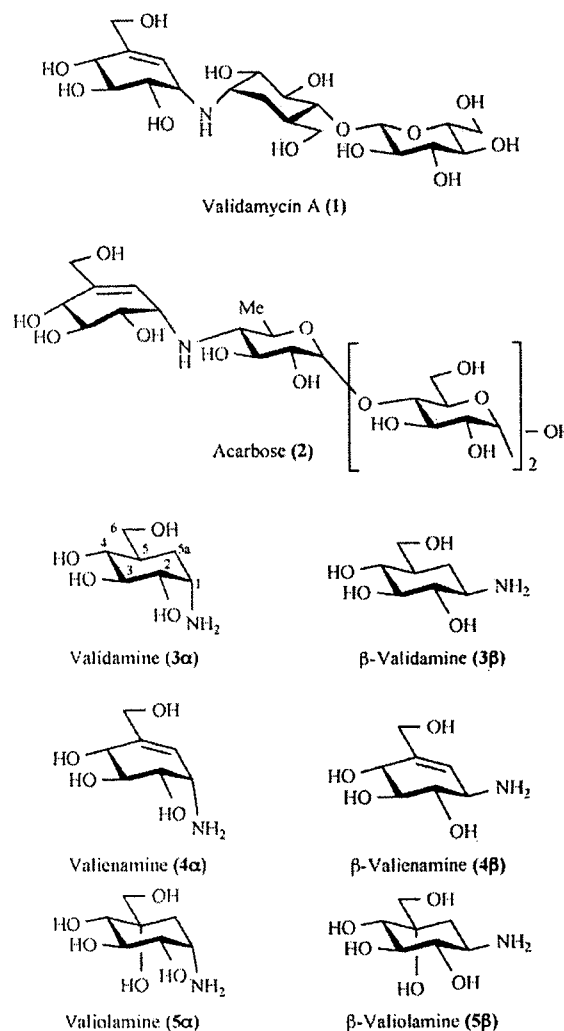
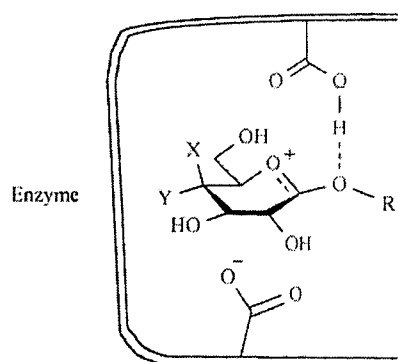


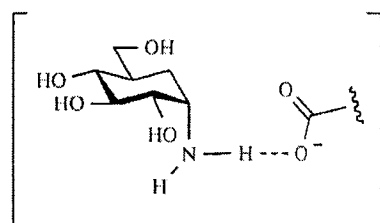
Fig. (1). Validamycin A and acarbose, and some naturally occurring 5a-carboglycosylamines **3 $\alpha$** –**5 $\alpha$**  and the 1-epimers ( $\beta$ -anomers) **3 $\beta$** –**5 $\beta$**  of biological interest.

\*Address correspondence to these authors at Department of Biosciences and Informatics, Faculty of Science and Technology, Keio University, Hiyoshi, Kohoku-ku, Yokohama, 223-8522 Japan; Tel: +81-422-49-5752; E-mail: sogawa379@ybb.ne.jp

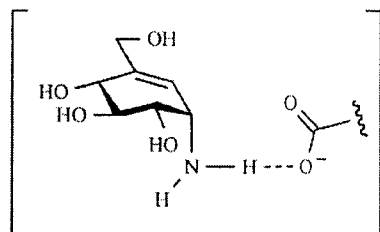
International University of Health and Welfare Graduate School, Kita-Kanemaru, Otawara, 324-8501 Japan; Tel/Fax: +81-287-24-3229; E-mail: SuzukiY@iuhw.ac.jp



Putative transition-state of hydrolysis of glycopyranosides (X = H, Y = OH) and galactopyranosides (X = OH, Y = H)



Ground-state  $\alpha$ -glucosidase inhibitor: validamine ( $3\alpha$ )



Transition-state  $\alpha$ -glucosidase inhibitor: valienamine ( $4\alpha$ )

**Fig. (2).** Hypothetical transition states for the cleavage of glycosidic bonds and binding of glycosidase inhibitors of 5a-carbaglycosylamine type to active sites of enzymes.

enzymes and to correct pathological intracytoplasmic storage of substrates in some human disorders. We therefore started a systematic survey of compounds exhibiting biological activity of this type, and found *N*-octyl-4-epi- $\beta$ -valienamine (NOEV) to be a good candidate for a new molecular therapeutic approach (chemical chaperone therapy), particularly to  $G_{M1}$ -gangliosidosis caused by  $\beta$ -galactosidase deficiency [8,9].

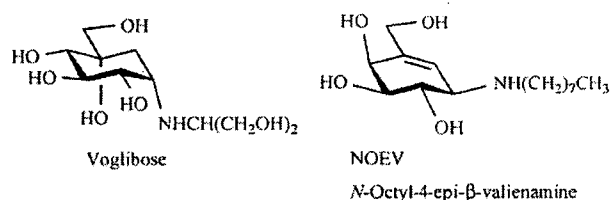


**Fig. (3).** Voglibose and NOEV.

## 2. DESIGN AND SYNTHESIS OF CARBAGLYCOSYLAMINE GLYCOSIDASE INHIBITORS

### 2.1. Structure-Inhibitory Activity Relationships

The active core of validamycin A (1), dicabadisaccharide validoxylamine A [10], resembles the substrate trehalose, the structure of which is thought to adopt a transition state for hydrolysis by trehalase. The unsaturated derivative of *N*-linked 5a,5a'-dicarba- $\alpha,\alpha$ -trehalose, composed of  $3\alpha$  and  $4\alpha$ , possesses strong inhibitory activity against trehalase [11]. On the other hand, the active core of  $\alpha$ -amylase inhibitor 2 is thought to be a maltose-type *N*-linked pseudodisaccharide, composed of  $4\alpha$  and 4-amino-4,6-dideoxy-D-glucopyranose.

Accordingly, by analogy with structure and inhibitory activity relationships deduced by consideration of the active compounds (1, 2, and  $3\alpha$ – $5\alpha$ ), the corresponding 5a-carbaglycosylamines (3 and  $6\alpha,\beta$ – $14\alpha,\beta$ ) and analogues with naturally common  $\beta$ -gluco,  $\alpha,\beta$ -galacto,  $\alpha,\beta$ -manno, and  $\alpha$ ,  $\beta$ -fuco-configurations [12] (Fig. 4), have been nominated as leads for development of new biological active compounds such as enzyme-inhibitors of structurally related glycosidases and/or glycosyltransferases.

### 2.2. Chemical Modification of Methyl Acarviosin

Acarviosin ( $15a$ ), the active core of acarbose (2) [13], is a very potent  $\alpha$ -glucosidase inhibitor, with activity attributable to structural features resembling the transition state associated with hydrolysis of maltose. We have attempted to ascertain the relationship between the stereochemistry of  $3\alpha$  and inhibitory activity against  $\alpha$ -glucosidase. Acarviosin was chosen as a suitable lead for this purpose, chemical modification of its aglycone portion being first carried out, giving the 6-hydroxyl derivative  $15b$  and two methyl ethers  $15c$ – $d$  [14] (Fig. 5). Decrease of inhibitory potency was observed for all derivatives prepared. However the 1,6-anhydride  $16a$  derived unintentionally by base-treatment of the 6-tosylate derivative of  $15b$  was found to possess activity as high as  $15a$  or greater [15]. Three dehydroxy derivatives  $16b$ – $d$ , obtained by consecutive removal of the hydroxyl groups of the anhydroglucopyranose residue, were found to have increased activity relative to decrease of hydrophilicity of the aglycone. These results suggested that improvement of the activity might be readily achieved by incorporation of simple hydrophobic functions of alkyl and phenylalkyl groups into the aglycone of  $3\alpha$ . Secondly, the 2'-epimer 17 of methyl  $\alpha$ -acarviosine was prepared [16], its unsaturated aminocyclitol part structurally in accord with an  $\alpha$ -mannopyranose residue. By analogy, pseudodisaccharide 17 was expected to show inhibitory activity toward  $\alpha$ -mannosidase, and was finally shown to be a mild  $\alpha$ -mannosidase inhibitor. On the same basis, two acarviosin analogues, the 1-epimer ( $18a$ ) and its 2-acetamido-2-deoxy derivative ( $18b$ ), were thus designed and synthesized [17]. Structures of their unsaturated aminocyclitol moieties corresponded to the postulated transition-state mimics of  $\beta$ -D-glucose and *N*-acetyl- $\beta$ -D-glucosamine residues, respectively, in hydrolysis of the respective glycosides. However, disappointingly, the pseudodisaccharides  $18a,b$  did not possess any inhibitory activity toward the respective commercially available  $\beta$ -glucosidase and chitinase forms.



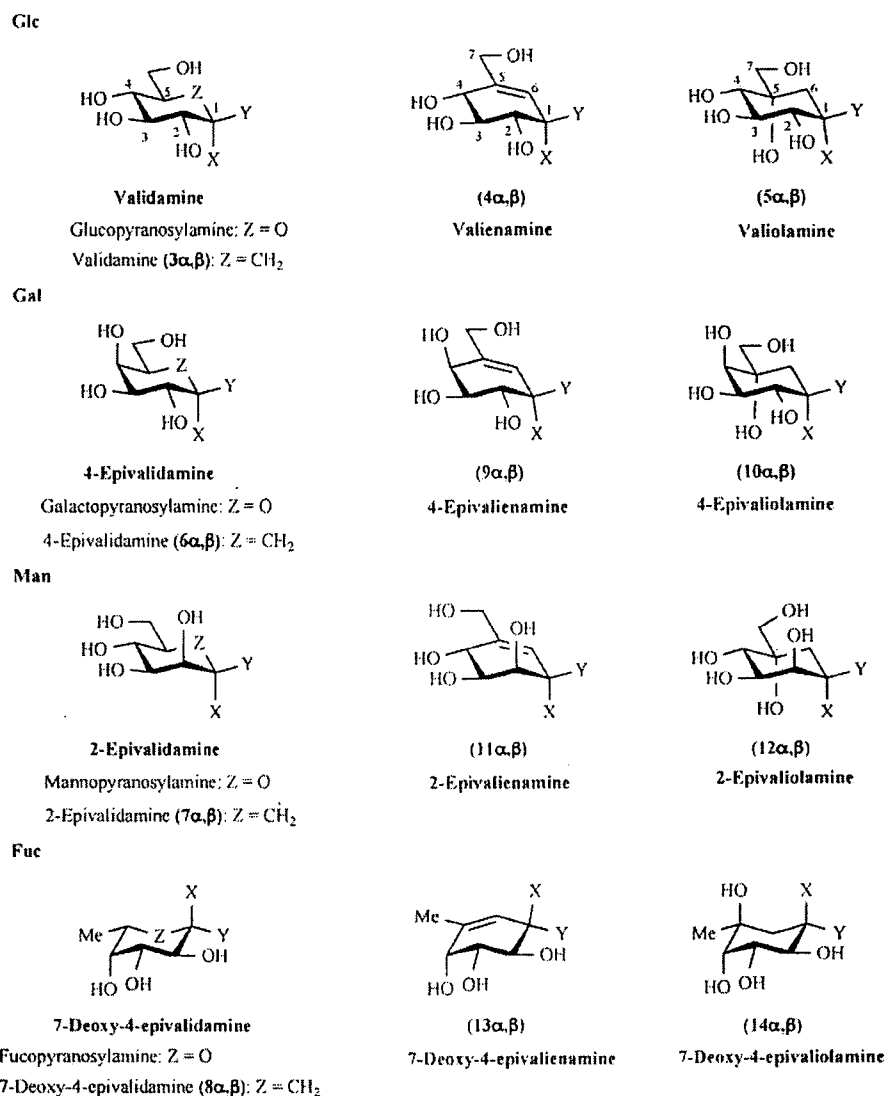


Fig. (4). Biologically interesting carbaglycosylamines and derivatives ( $\alpha$ : X = NH<sub>2</sub>, Y = H;  $\beta$ : X = H, Y = NH<sub>2</sub>).

### 2.3. Design and Synthesis of Carbaglycosylceramides

In 1991, some glycosylamides **19a** were demonstrated [18] to possess significant potential as immunomodulators of responses to *Escherichia coli* (Fig. 6). We therefore became interested in ready preparation of glycosylamide analogues, the sugar moieties being replaced with carbasugars, the resulting *N*-(5 $\alpha$ -carba- $\beta$ -glucopyranosyl)-*N*-octadecyl-dodecanamide (**19b**) and related carbasugar analogues [19] possessed similar biological activity to true sugar congeners and we therefore anticipated development of biologically interesting carbasugar derivatives for basic research into glycolipids. Referring to natural occurring glucosyl and galactosylceramides, we first elaborated a total synthesis of 5 $\alpha$ -carbaglucosylceramides **20a-c**, where 5 $\alpha$ -carba- $\beta$ -D-glucopyranose residues were bonded to ceramide-chains through ether, thioether, and imino linkages, respectively [20]. Among the carbaglycosylceramides obtained, the *N*-linked analogue **20c**, together with the galactosyl analogue **21** later provided, were

observed to possess weak but distinct inhibitory activity against the corresponding gluco and galactocerebrosidases (mouse liver). Encouraged by these results, incorporation of unsaturated-bonds into the carbasugar residues was attempted in the hope of increasing their potential and selectivity. Carbaglycosylceramide analogues **22a** and **22b**, featuring valienamine and its 4-epimer, were thus prepared and demonstrated to have very potent and specific inhibitory activity (IC<sub>50</sub> 0.3 and 2.7  $\mu$ M) toward the respective gluco and galactocerebrosidases [21] (Fig. 6). The configuration at C-4 of the valienamine moiety was found to be a critical point for differential recognition by the respective enzymes, as with gluco and galactopyranose residues.

### 2.4. Modification of Carbaglycosylceramides: Synthesis of Potent $\beta$ -Gluco and Galactocerebrosidase Inhibitors

The above lead compounds thus made possible our aim of structurally more simple carbaglycosylceramide analogues with high potency.

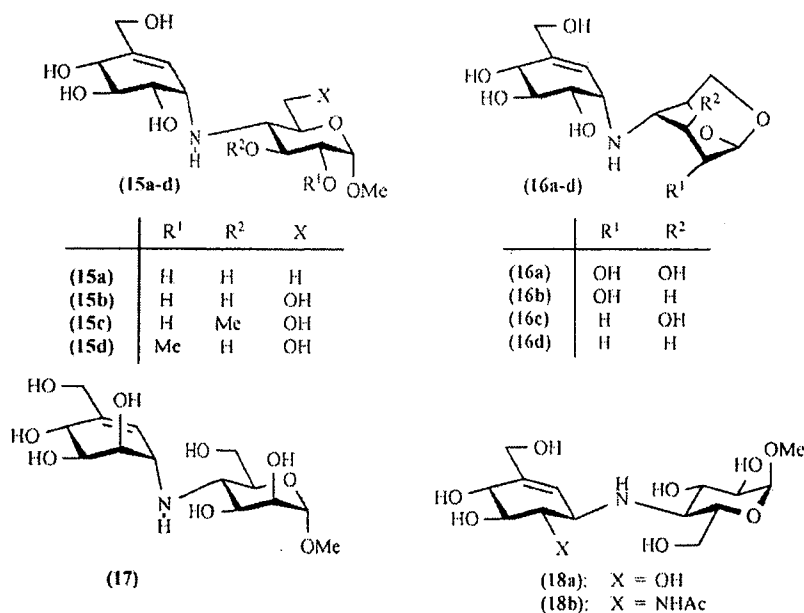


Fig. (5). Chemical modification of methyl acarviosin (15a).

Several *N*-alkyl- $\beta$ -valienamines **23a–d,f,h** were designed and prepared systematically to determine, if possible, any relationship between chain length of aliphatic functions and inhibitory activity [22] (Fig. 6). Actually, the *N*-octyl derivative **23c** was found to possess about 10-fold greater potency

than the parent carbaglusylceramide **22a**, indicating the possibility of replacing the ceramide moiety by simple hydrophobic aliphatic chains without affecting the activity (Table I). Similarly, some double-strand type *N,N*-dialkyl derivatives **24a–g**, prepared by reduction of the corresponding

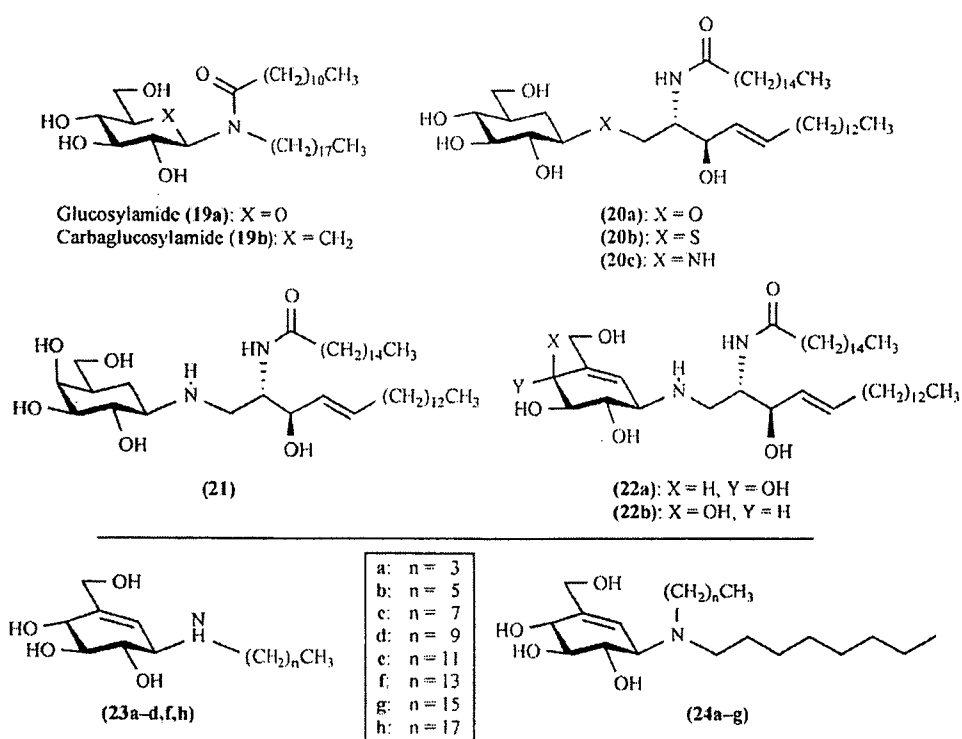


Fig. (6). 5a-Carbaglusyl and galactosylceramides, and some *N*-alkyl- and *N,N*-dialkyl- $\beta$ -valienamines.

**Table 1. Inhibitory Activity ( $IC_{50}$ ,  $\mu M$ ) of Some *N*-Alkyl- $\beta$ -valienamine Homologues Against  $\alpha$ -Glucosidase (Baker's Yeast) and  $\beta$ -Glucocerebrosidase (Mouse Liver)**

| Compound   | $\alpha$ -Glucosidase | Glucocerebrosidase |
|------------|-----------------------|--------------------|
| 3 $\alpha$ | 100                   | NI                 |
| 3 $\beta$  | 100                   | NI                 |
| 22a        | NT                    | 0.3                |
| 23a        | NI                    | 11                 |
| 23b        | 50                    | 0.3                |
| 23c        | 17                    | 0.03               |
| 23d        | NT                    | 0.07               |
| 23f        | NT                    | 0.12               |
| 23h        | NI                    | 0.3                |

NI: No inhibition ( $<10^{-3}$  M); NT: Not tested.

alkylamide derivatives, were also revealed to be as potent as their parents [23]. However, we were rather disappointed by the unexpected fact that *N*-octyl-4-epi- $\beta$ -valienamine (26b) [8] prepared at the same time did not show any significant improvement in potency toward galactocerebrosidase. On the other hand, interest in studying actions of inhibitors toward glycosidases and glycosyltransferases prompted us to provide hybrid-inhibitors with functions targeting inhibition of both glucosylceramide synthase and glucocerebrosidase under controlled conditions. Thus, PDMP ( $IC_{50}$  23  $\mu M$ , mouse liver) [24] was chosen as a potent synthase-inhibitor, and coupling of all stereoisomers of PDMP with carbamaglycosylamines 3 $\beta$ , 4 $\alpha$  and 4 $\beta$  via N-linkages afforded four respective *N*-(2-decylamino-3-hydroxy-3-phenylprop-1-yl)- $\beta$ -valienamines 25a-c [25] (Fig. 7). Interestingly, all coupled compounds were shown to be strong  $\beta$ -glucocerebrosidase inhibitors, while the PDMP moiety abrogated activity against

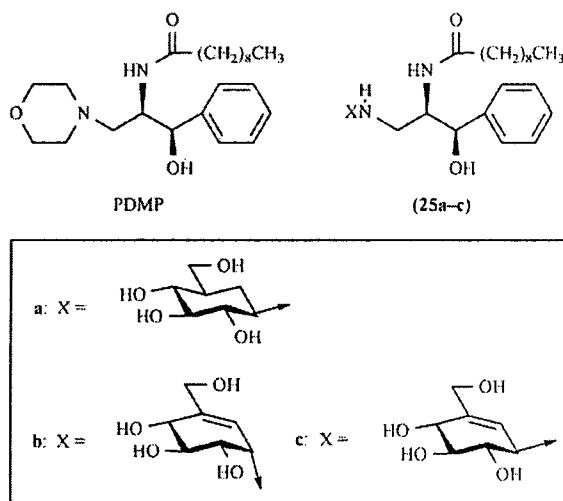


**Fig. (7).** The glucosylceramide synthase inhibitor PDMP and its hybrids composed of 5a-carbamaglycosylamines.

glucosylceramide synthase: e.g. 25c corresponding to the (2*R*,3*R*)-isomer of PDMP possessed inhibitory activity  $IC_{50}$  0.7  $\mu M$  against glucocerebrosidase (mouse liver).

After almost two years, strong and specific inhibitory activity ( $IC_{50}$  0.3  $\mu M$ , human  $G_{MI}$   $\beta$ -galactosidase) was observed for *N*-octyl-4-epi- $\beta$ -valienamine (26b), which was then selected as a new candidate for chemical chaperon therapy of human genetic diseases [9]. Taking advantage of the available data, we have concentrated our efforts on developing effective synthetic routes to 4-epi- $\beta$ -valienamine derivatives in order to facilitate screening of as many homologous compounds as possible [26] (Fig. 8). Inhibitory assay results for four such homologues 26a-d thus prepared are listed in Table 2.

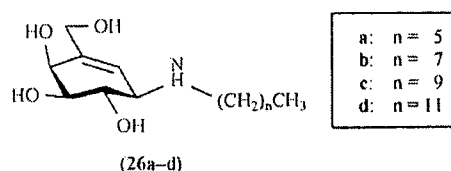


**Fig. (8).** Some *N*-alkyl-4-epi- $\beta$ -valienamines.

## 2.5. Structure-Inhibitory Activity Relationships of Unsaturated Carbamaglycosylamine Glycosidase Inhibitors

Free glycosylamines as well as *N*-alkyl derivatives, namely, simple *N*-glycosides, are often chemically unstable in aqueous solution, undergoing mutarotation accompanied by hydrolytic cleavage to give rise to equilibrium mixtures of sugars and ammonia or amines [27]. Since carbamaglycosylamines are comparatively stable polyhydroxylated (hydroxymethyl)cyclohexylamines, they might be expected to play roles as non-hydrolyzable mimics of glycopyranosylamines of biological interest. Taking advantage of their chemical and biochemical features, preferential utilization as active lead compounds in biological systems and/or building blocks of complex glycoconjugate molecules has been targeted. Moreover, in addition to the chemical stability, efficient modification of the stereochemical nature of carbamaglycosylamines may be achieved by unsaturation at C-5 and C-5a, hydroxylation at C-5 and/or C-5a, and so on (as seen in Fig. 4), without appreciably altering their characteristic features as close mimics of particular hexopyranoses, possibly leading to improvement of biological potential.

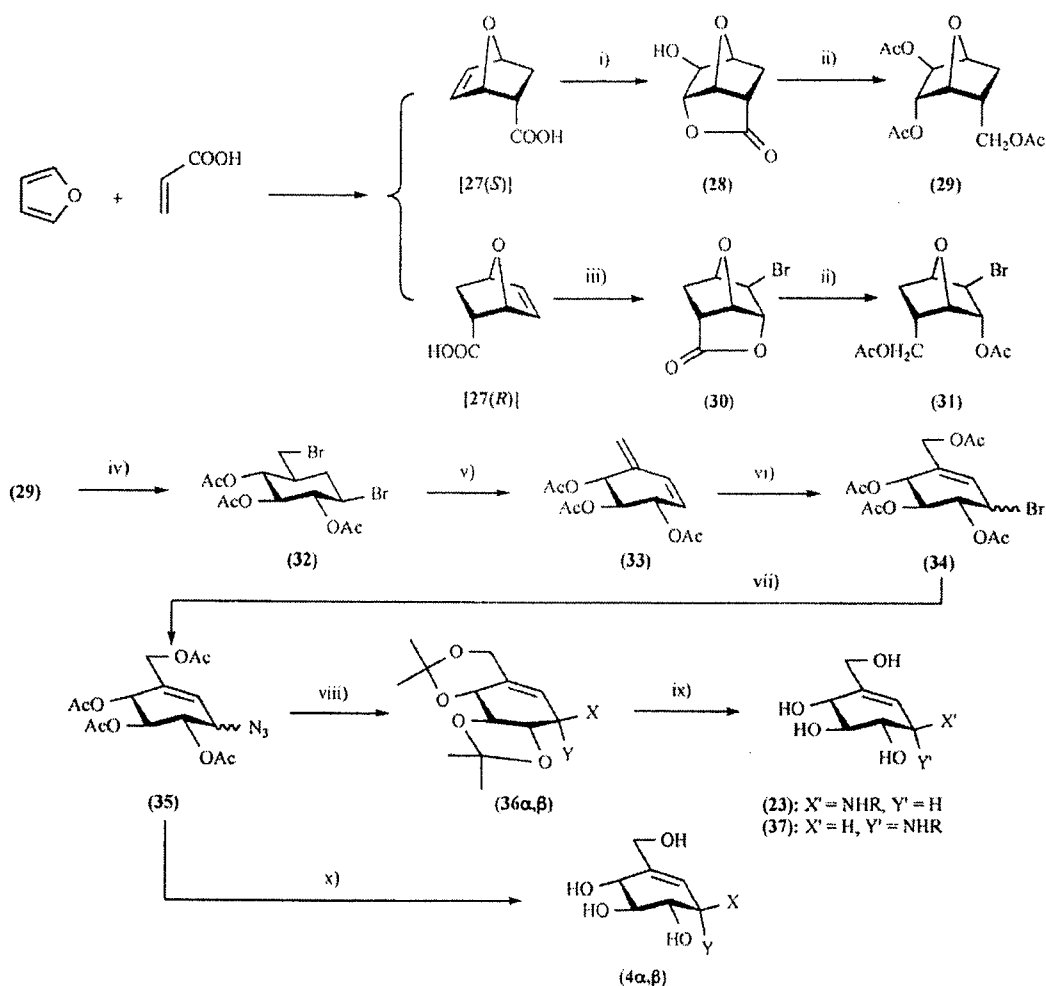
As shown by the inhibitory activity of 4-epi- $\beta$ -valienamines (9 $\beta$ ) and the *N*-alkyl derivatives 23a-d (Table 2), inclusion of hydrophobic *N*-alkyl chains into 9 $\beta$ , is very important for improving its potential significantly, which would suggest that, in attempts to develop new such analogues and mimics, additional modification of their physicochemical nature might be advisable, for instance for the purpose of generating strong binding to active sites of enzymes or peptides. With 4 $\beta$  and 9 $\beta$ , our present knowledge suggests that a simple eight-carbon chain may be sufficient.

## 2.6. Novel Synthetic Routes to Carbamaglycosylamines of Biological Interest

Valienamines (4 $\alpha$ , $\beta$ ) were first totally synthesized [28] from the conjugate alkadiene (33), derived from the *endo*-adduct 27(*S*) of furan and acrylic acid (Fig. 9). Di-*O*-iso-

**Table 2.** Inhibitory Activity (IC<sub>50</sub>, μM) of 4-Epi-α- and β-valienamines 9α,β, and Some *N*-Substituted Derivatives 26a-d Against Four Glycosidases

| Compound | α-Glucosidase <sup>a</sup> | β-Galactosidase <sup>b</sup> | β-Glucosidase <sup>c</sup> | α-Mannosidase <sup>d</sup> |
|----------|----------------------------|------------------------------|----------------------------|----------------------------|
| 9α       | 56                         | NI                           | NI                         | 370                        |
| 9β       | 12                         | NI                           | NI                         | 190                        |
| 26a      | 207                        | 2.3                          | 1.2                        | NI                         |
| 26b      | 3.1                        | 0.87                         | 3.1                        | NI                         |
| 26c      | 1.9                        | 0.13                         | 2.5                        | NI                         |
| 26d      | 4.4                        | 0.01                         | 0.87                       | NI                         |
| DMJ      | NT                         | NT                           | NT                         | 150                        |

NI: No Inhibition (>10<sup>-3</sup> M); NT: Not tested.<sup>a</sup>Green Coffee Beans; <sup>b</sup>Bovine liver; <sup>c</sup>Almonds; <sup>d</sup>Jack Beans.**Fig. (9).** Synthesis of 5a-carbaglycopyranosylamines with β-*gluco* configurations, starting from the Diels-Alder *endo*-adduct of furan and acrylic acid (α: X = H, Y = NH<sub>2</sub>; β: X = NH<sub>2</sub>, Y = H). Conditions and reagents: i) H<sub>2</sub>O<sub>2</sub>, HCOOH; ii) LiAlH<sub>4</sub>/THF; Ac<sub>2</sub>O/Py; iii) Br<sub>2</sub>, NaHCO<sub>3</sub>/H<sub>2</sub>O; iv) 15% HBr/AcOH, 80 °C; v) DBU/toluene; vi) Br<sub>2</sub>, AIBN, AcOH; AcONa, aq. MCS; vii) NaN<sub>3</sub>/aq. DMF; viii) NaOMe/MeOH; DMP, *p*-TsOH/DMF; H<sub>2</sub>S, or Ph<sub>3</sub>P/aq. *p*-dioxane; ix) RCOCl/Py; LiAlH<sub>4</sub>/THF; aq. AcOH; acidic resin treatment; x) NaOMe/MeOH; H<sub>2</sub>S, aq. DMF.